RELAXATION STUDIES OF THE SULFATE AND NITRATE COMPLEXES OF THE LANTHANIDES AND U(VI) IN AQUEOUS SOLUTION

By

DANIEL LITCHINSKY

Bachelor of Science

University of Alberta

Calgary, Alberta, Canada

1965

Submitted to the Faculty of the Graduate College
of the Oklahoma State University
in partial fulfillment of the requirements
for the Degree of
MASTER OF SCIENCE
May, 1968

RELAXATION STUDIES OF THE SULFATE AND NITRATE COMPLEXES OF THE LANTHANIDES AND U(VI) IN AQUEOUS SOLUTION

Thesis Approved:

Neil Purdie
Thesis Adviser

Horacio A Mottola

Tom E. Moore

N Durham
Dean of the Graduate College

PREFACE

This study was done in answer to a criticism of a paper on ultrasonic absorption in the lanthanide sulfates by N. Purdie and C. A. Vincent. The argument that the absorption of the lanthanide sulfates is a cation dependent process cannot be concluded until a study of anion dependence is done. The nitrates of the lanthanides are studied and compared with the corresponding sulfate.

Uranyl sulfate and uranyl nitrate are studied to determine whether the relaxations observed are due to complex formation or hydrolysis.

I wish to express my gratitude to Professor N. Purdie, research adviser, for his invaluable guidance, patience and confidence during the preparation of this thesis. Thanks are due Mr. Douglas P. Fay who prepared the sulfates of the lanthanides for this study. I also wish to thank Dr. T. E. Moore for aid and assistance during the course of my graduate work at Oklahoma State University.

TABLE OF CONTENTS

LIST OF TABLES

LIST OF FIGURES

LIST OF FIGURES (Continued)

CHAPTER I

INTRODUCTION

The properties of aqueous solutions of electrolytes depend, for the most part, on ion-water interactions as described in the model of Frank and Wen[1]. The ions at infinite separation are surrounded by three concentric regions:

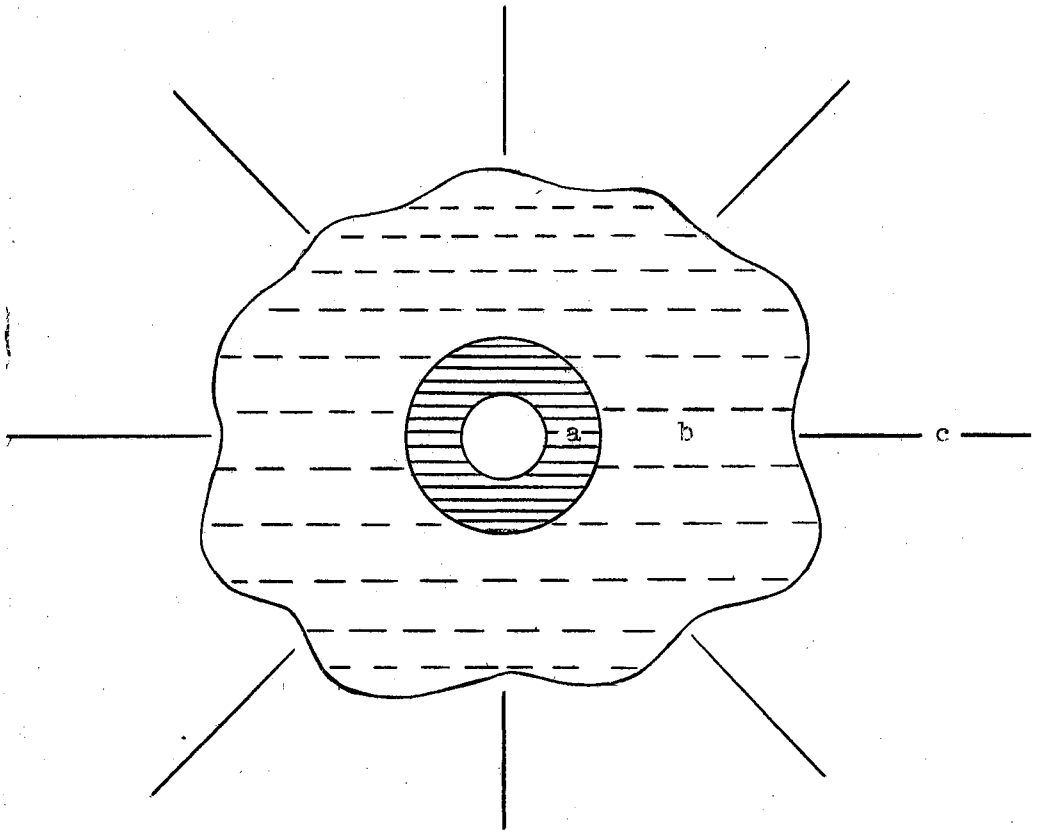

Figure 1. The Hydrated Ion

a primary or inner sphere (a) of strongly bound water molecules, a second sphere (b) with water molecules still ordered to some extent by electrostatic forces of polarization and a third sphere (c) having water influenced only slightly by the presence of the ion and essentially resembling the structure of the pure solvent. At short interionic distances the coulombic attraction of ions of opposite charge can bring about substitution of ions for solvent molecules in the first and second hydration spheres. The species produced are called ion pairs, outer ion pairs if solvent molecules exist between the ions and inner ion pairs or complexes if the ions are in contact. Studies of the thermodynamics of ion pair formation by classical methods such as conductivity measurements, spectrophotometry, polarography, potentiomentry and solubility measurements have been unable to distinguish between these species.[2] This is not unreasonable since, using the present model, the species existing in equilibrium could not be resolved due to the complexity of the system, Figure 2.

Two processes are involved in the first step between states 1 and 2. First, the free hydrated ions approach each other to within the approximate dimensions of their ionic atmospheres, and second, there is a rearrangement of ions and molecules within the ionic atmosphere to give structure 2. The second step is the loss of a water molecule from the primary coordination sphere of the anion. The anion has three modes of interaction with the water molecules of the cation. The anion may interact strongly with one hydrogen of a water molecule in the primary hydration sheath of the cation, or with two hydrogens on either the same or two adjacent water molecules. At any one time the three structures are in equilibrium with one another. The third step is

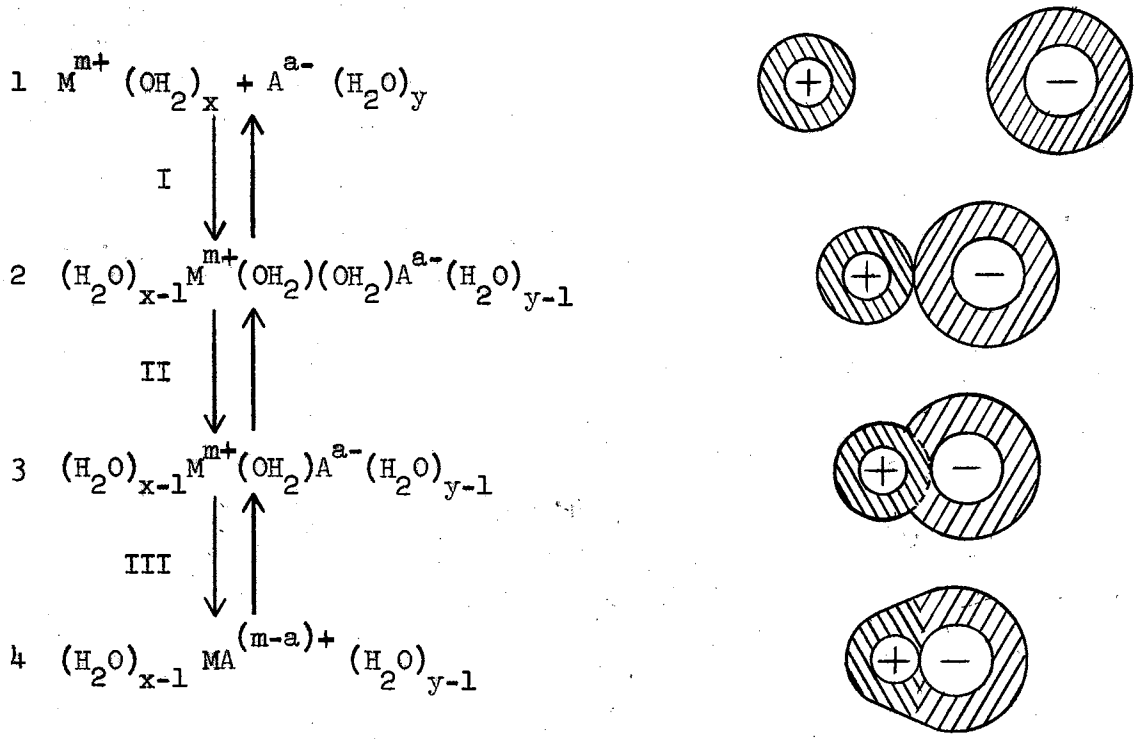

Figure 2. Mechanism of Ion Pair Formation

the replacement of a water molecule from the inner coordination sphere of the cation by the anion and the formation of a chemical bond between the ions. There is a concomitant increase in the degree of disorder of the water structure as a result of charge neutralization and this gain in entropy is very often the principal contributing factor to thermodynamic stability. This is particularly true in the case of unsymmetrical electrolytes in which the various states have a net charge.

If the equilibrium constants for the various reactions in the mechanism are K_I, K_{II} and K_{III}, then the overall stability constant K_T can be shown to be

$$K_T = \frac{1+K_{III}+K_{II}K_{III}}{K_I K_{II} K_{III}} \qquad (1)$$

As a consequence, the structure of the complexed species present in solution can not be identified by the overall stability constant. The utility of the conventional approach is limited to situations wherein the anion, for example, is kept constant and the change in K_T for a series of complexes with similar metal ions is a function of the cationic properties and therefore of K_{III}. It is apparent from equation (1) that a simple relationship does not exist between the various equilibrium constants and consequently, extreme caution must be used in drawing conclusions about the predominant species in solution from stability measurements alone. If heat and entropy data are available, the conclusions are more justified.

The only route to the evaluation of the individual equilibrium constants is by kinetic measurements. Equilibrium is reached very rapidly and the problem is amenable only to modern relaxation methods. The complete mechanism, rewritten to introduce the rate constants

$$\begin{array}{ccc} M^{m+}(aq) + A^{a-}(aq) & \underset{k_{21}}{\overset{k_{12}}{\rightleftharpoons}} & M^{m+}(H_2O)(H_2O)A^{a-} \\ & & \Big\uparrow_{k_{32}} \quad \Big\downarrow_{k_{23}} \\ H_2O + MA^{(m-a)+} & \underset{k_{43}}{\overset{k_{34}}{\rightleftharpoons}} & M^{m+}(H_2O)A^{a-} + H_2O \end{array} \qquad (2)$$

shows a dependence of $K_{III} = k_{34}/k_{43}$ on the ratio of the concentrations of inner to outer complex.

Evidence indicates that the rate determining step of the mechanism is indeed step III. Supporting this are several theoretical considerations:

(a) If the rates of diffusion of the aquated ions, to within two water molecules of each other, are calculated from the theory of diffusion controlled reactions, the relaxation time should lie in the order of 10^{-9} seconds.

(b) The ease of removal of water molecules from an oxyanion should take place faster than from a corresponding cation since the interaction of the anion with the surrounding water molecules is usually weaker than for the cation.

(c) The waters coordinated to the cation should be held more strongly due to the large surface charge on the cation resulting from the small ionic radius.

Experimental evidence for the correlation of the slow step with step III is exhibited by the dependence of the rate on the cation for a series of similar 1:1 and 2:2 electrolytes.[3] Sulfate, EDTA and NH_3 complexes of Cu, for example, are formed at nearly the same rate.[3] D_2O studies of complexation show no dependence of OH bonds on the observed relaxations.[4] That the rate constants are directly related to step III has been confirmed by Connick[5] in a number of studies using O^{17} labelled water in NMR studies of water exchange rates in the transition elements. The rates obtained are related to $^{17}OH_2$ molecules entering the first coordination shell of the paramagnetic cations. The rates of water exchange for the divalent ions when compared with

Eigen's[3] values for the rates of formation of inner sulfate ion pairs show a fairly close parallelism.

Since the substitution rate is apparently independent of the nature of the entering ligand, the metal to water bond must be broken prior to the arrival of the ligand at the coordination site. Such a mechanism is designated S_N1. This explanation is consistent with the observation that the slow step is cation dependent.

The rates of complex formation of the alkali metals, the alkaline earth metals and the transition metals closely follow changes in electronic structure. This can be seen from the plots of log k_{34} vs $1/r$ for the alkali and the alkaline earth metals which give a linear rate dependence, as would be assumed for ions of noble gas configuration. For the transition metals the rates follow the effects of ligand field stabilization as seen in Figure 3.

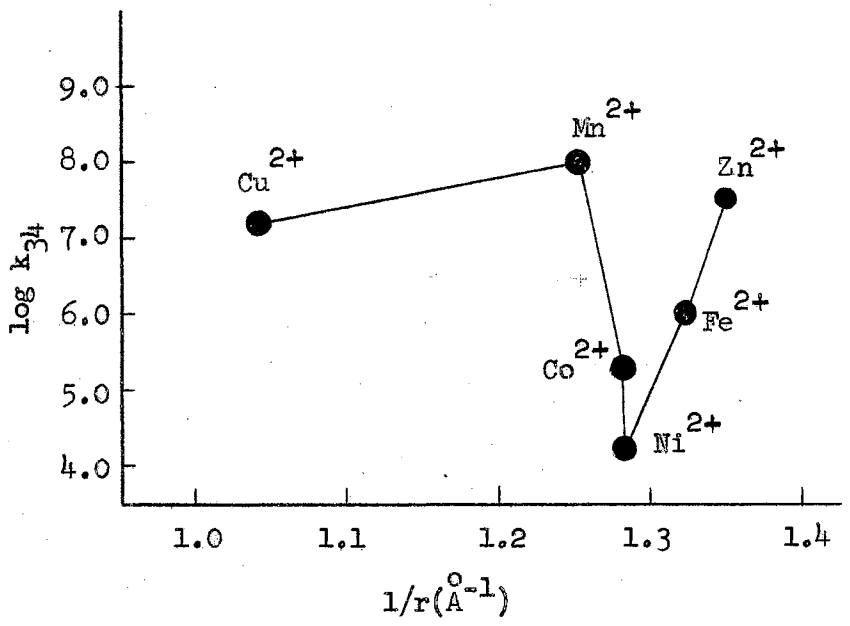

Figure 3. log k_{34} vs $1/r$ for the Transition Metal Series[3]

The ligand field effects on the stability of the trivalent rare earth complexes and on the rates of ligand substitution are considered small because of the deep penetration of the 4f electrons into the electronic atmosphere of the ion--a maximum of 10% contribution to the stability has been suggested by Dunn.[6] It is reasonable, therefore, to expect them to behave like the alkaline earth metals because of their pseudo-noble gas configuration. That they do not, Figure 4,

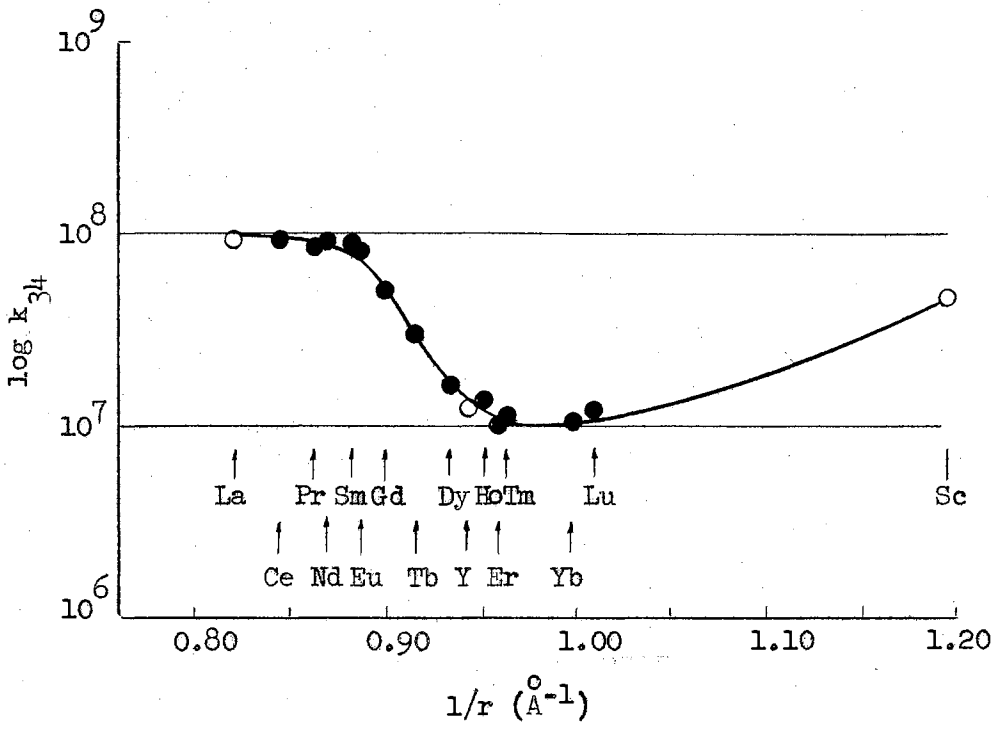

Figure 4. Log k_{34} vs 1/r for the Rare Earth Metals (from Geier[7])

has been attributed to a change in hydration or coordination number of the series. Entropy studies by Yatsimirskii[8] have shown a range in

the lanthanide series where the entropy of complexation changes abruptly and it is possible to associate this with two forms of coordination which differ with the atomic number of the metal.

There is at least one exception to the independence of the slow step on the nature of the ligand. This arises in hydrolysis reactions where, depending upon the pH, the "entering" group will be either a hydroxide ion or a water molecule. If the rate of substitution of water is slower than the rate of proton transfer from the primary coordinated water to the "entering" group, then the rate controlling step in basic medium will be:[9,10]

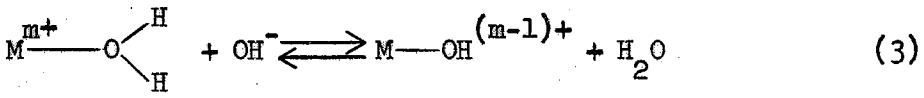

(3)

and in an acid medium:

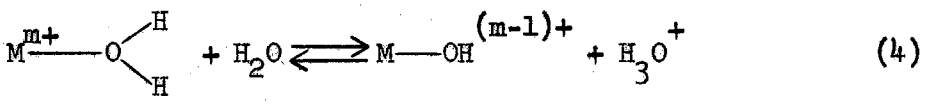

(4)

Hydrolysis reactions can complicate studies of complex formation especially when the cation is relatively small and highly charged, for example Al^{3+}, Be^{2+}, Fe^{3+}, U(VI), and in particular when stable polynuclear complexes are produced.

General Theory

In 1950 relaxation methods for studying rapid reactions in solution were introduced by M. Eigen.[11] The principle of these methods is the variation of some external parameter of a system at or near equilibrium. The parameters varied can be temperature or pressure.

For example, if the chemical equilibrium is temperature dependent, the concentrations will all change from their equilibrium values at T_1 to their respective values at T_2. The rates at which the concentrations change from one equilibrium state to another is a consequence of the kinetics of the opposing reactions. Any type of perturbation can be used if it causes a measurable change in concentration from some arbitrary reference state; examples are step-function perturbations, periodic perturbations and pulsed perturbations.[12]

Four relaxational methods have been used extensively: temperature jump, pressure jump, the II Wein effect (electric field jump) and ultrasonic absorption. In the present study pulsed ultrasound was used.

Relaxation methods have a unique feature. Since the deviations from an equilibrium state are very small, the kinetics of a system can be described by a set of linear differential equations. For example, in the general reaction

$$A + B \underset{k_{-1}}{\overset{k_1}{\rightleftharpoons}} AB \qquad (5)$$

the rate equation is:

$$-\frac{d\Delta c}{dt} = \frac{1}{\tau}\Delta c \qquad (6)$$

where Δc is the deviation of the concentration of all components from their equilibrium values and τ is called the relaxation time of the system. If the chemical system is complex, a system of rate equations of the general form,

$$\frac{d\Delta c}{dt} = \Sigma\, a_{ij}\, \Delta c_j \qquad (7)$$

are obtained where a_{ij} are known functions of rate constants and equilibrium concentrations. If the system of simultaneous equations is solved, a spectrum of relaxations is obtained--each relaxation time having its own particular dependence on the equilibrium concentrations.

An ultrasonic wave propagates as an adiabatic pressure wave. Both temperature and pressure changes accompany the sound wave but in aqueous solutions, temperature fluctuations are nearly absent because the thermal expansion of H_2O is very small (zero at $4^{\circ}C.$). The adiabatic compressibility of the fluid may be resolved into a virtually instanteous portion plus a time dependent portion:

$$\beta = \beta_r' + \beta_\infty \qquad (8)$$

where β_∞ is the instantaneous compressibility and is given by the limiting value as the frequency approaches infinity.

β_r' is the relaxational part of the compressibility which is frequency dependent.

If the frequency of pressure variation in the liquid is low, then the chemical equilibrium is continuously maintained and the volume-pressure relationship will be the static one β_∞. On the other hand, if the frequency of pressure variation is very large, then the chemical equilibrium cannot be greatly altered during the pressure change. Between these two frequency limits lies the region of absorption. Since the system cannot immediately re-establish equilibrium with a pressure rise as in case 1, it follows that a phase lag exists between pressure and the specific volume. The frequency dependence of the

relaxational compressibility is

$$\beta_r' = \beta_r/(1+w\tau) \tag{9}$$

where w is the angular frequency.

β_r is a real number.

The phase lag causes dissipation of energy with each cycle

$$\text{Energy Lost Per Cycle} = \oint PdV \tag{10}$$

As the frequency rises from a low value, the shift in equilibrium will increasingly lag behind the pressure. The maximum energy is lost when:

$$(\alpha\lambda)_r = \frac{\pi\beta_r}{\beta_o}\left(\frac{w\tau}{1+w^2\tau^2}\right) \tag{11}$$

where $\beta_o = \beta_r + \beta_\infty$

α excess absorption per wave length

τ is the relaxation frequency

w is angular frequency

The maximum occurs at a frequency of $w = \frac{1}{\tau}$. This yields an absorption curve Figure 5, which is independent of frequency.

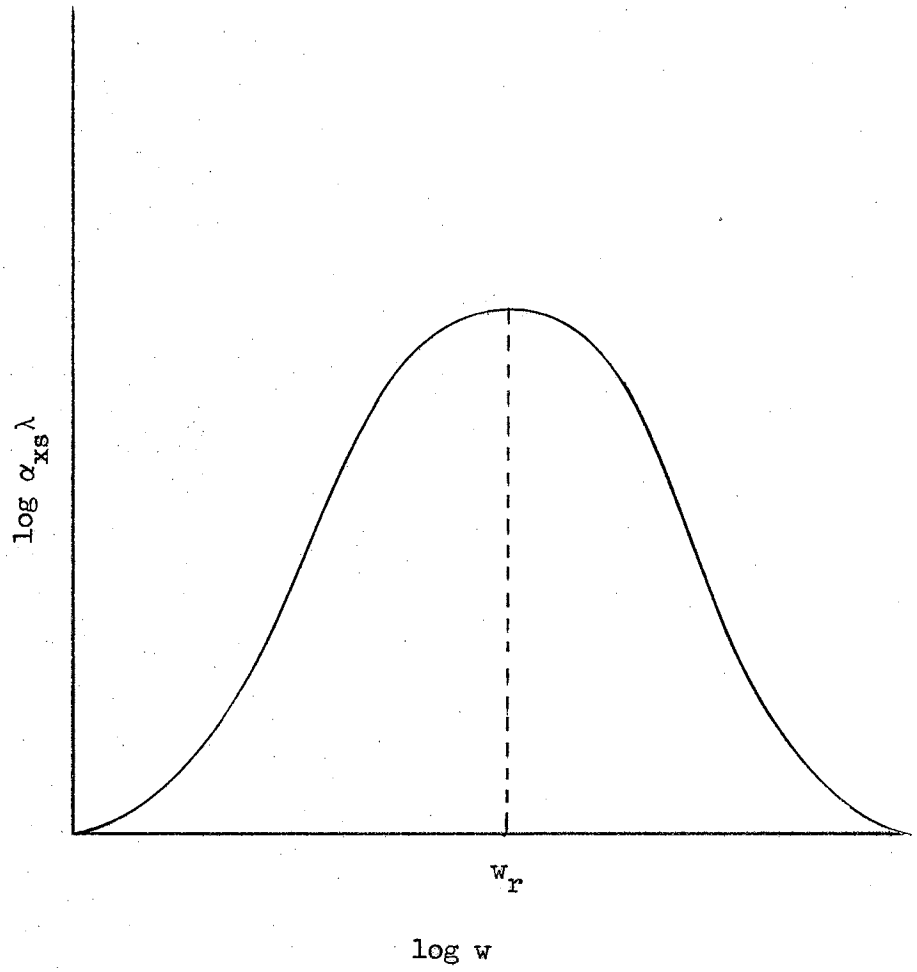

Figure 5. Ultrasonic Absorption Plot

CHAPTER II

APPARATUS

The pulse technique can be used in the frequency range 1-300 MHz. Since the absorption is proportional to the square of the frequency, the absorption is very small below 1 MHz. At very high frequencies, the efficiency of the crystal transducer is greatly reduced. The equipment used in this study has a frequency range of 5 to 75 MHz.

The Electronic System

A block diagram of the apparatus is shown in Figure 6. The signal is initiated by a square wave pulse generator supplying two output pulses at about 60 pulses per second which are separated by a variable delay. The two pulses are similar in amplitude and polarity and are therefore identical. The first pulse drives a pulse amplifier which supplies approximately 500 volts amplitude to the transmitters. These in turn put out 150 volts peak to peak into a circuit impedance of 75 ohms to drive a crystal transducer. The second pulse drives a transistor pulse amplifier. This pulses a particular comparison pulse oscillator, and the output from the selected unit is passed through a set of precision attenuators. The outputs of the receiving transducer and the attenuators are combined in a passive addition circuit and taken to a video amplifier. The resultant signal is then displayed on an oscilloscope, Tektronix 536, equipped for fast rise time.

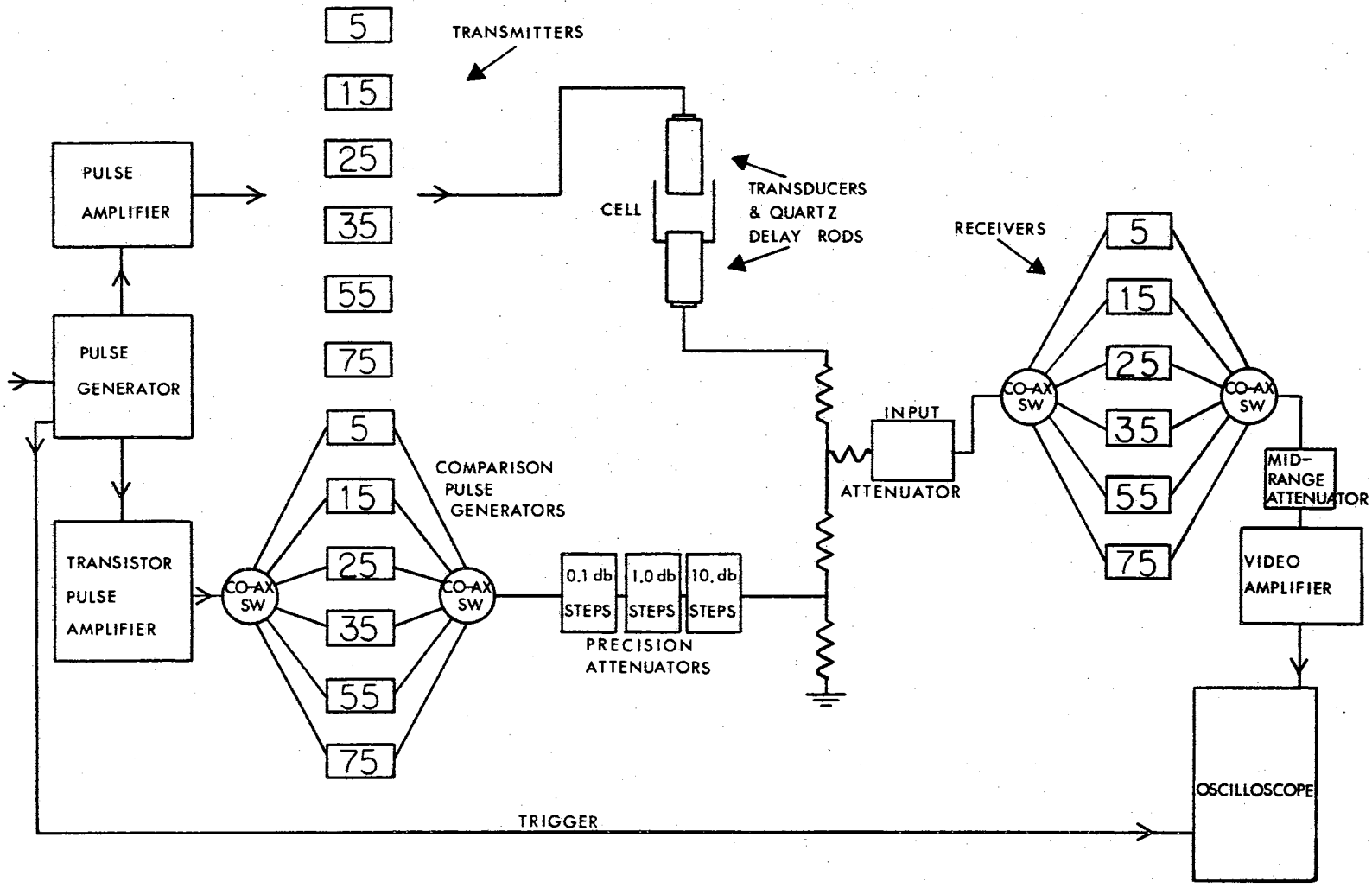

Figure 6. Block Diagram of the Electronic Apparatus

The Mechanical System

The mechanical system is picture in Figure 7. It consists of three parallel stainless steel platforms anchored to a stainless steel back. On the lower platform is positioned a table, fastened by a spring through the center and two spin off nuts on either side. The table is supported by three adjustable levelling feet. The table is actually a large chuck into which a quartz rod can be inserted, electrical contacts with the rod being made on the sides of the chuck and through the bottom by a spring leaf assembly; the external connection is made through a BNC connector mounted on the side of the table. The center platform has a moveable chuck (electrical connections through the sides and base) tensioned by springs so as to maintain position if moved vertically. The upper platform has a micrometer firmly mounted above the upper chuck. The micrometer moves the upper chuck through an intermediate stainless steel ball to achieve calibrated vertical motion of the receiver transducer.

The Transducer Assembly

Two delay rods of Spectrosil B grade fused quartz were obtained from Thermal Syndicates Ltd., England. The emitter and lower rod has the specifications, length--80 mm$\pm$1.0mm, diameter--30mm$\pm$0.5mm, one end ground to a taper, the semi angle being 5 degrees leaving the diameter of one end 24mm. The tapered end fits a water jacket. The detector rod dimensions are 80$\pm$1mm in length and 20mm$\pm$0.5mm in diameter. Both cylinders have end faces optically flat to 1/4 of the wave length of green light and are parallel to 6 seconds of arc.

Each rod was platinum plated on one end and to approximately 30mm

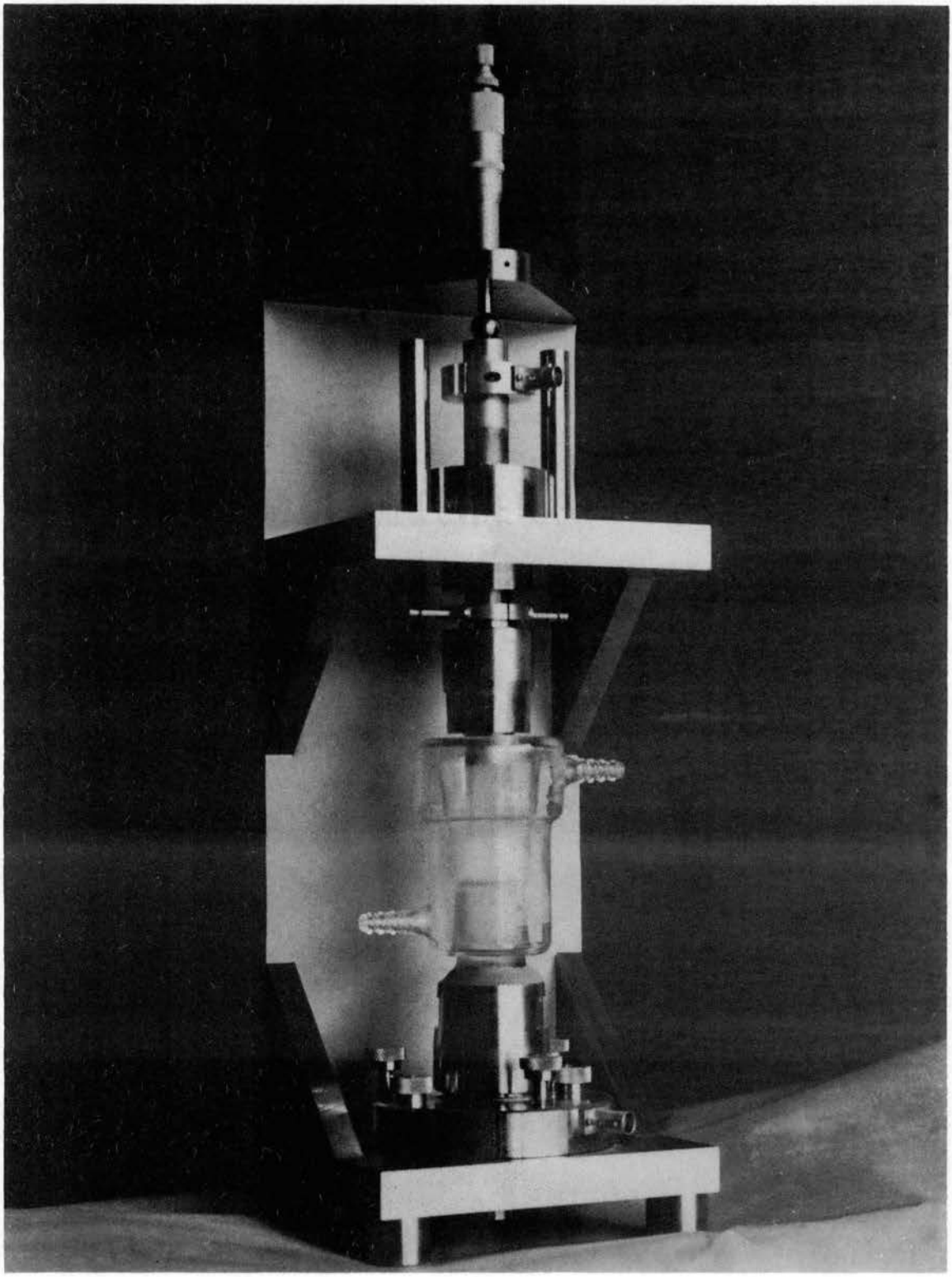

Figure 7. Mechanical System

along the side by repeated application and heating to 700°C of Liquid Bright Platinum (DuPont #7447) until a conducting surface of approximately 1 ohm resistance between face and side was achieved.

The piezoelectric transducers are X-cut crystals with a fundamental resonant frequency of 5000 KHz with a tolerance of ±70 KHz (Marconi's W. T. Co. Ltd.). The crystals were attached to the delay rods using hot paraffin wax--the crystals being "set in" until there was essentially a monomolecular bond between the crystal and rod. The outer face of the crystal was coated with liquid silver conducting paint to achieve electrical contact. The rods were checked for excess attenuation due to poor bonding and the "setting in" process repeated until the lowest value of attenuation was obtained.

Experimental Procedure

The solution under study was placed in the thermostated cell. The delay rods were made parallel by adjusting the lower table until the first pulse displayed on the oscilloscope was maximized. This was usually done at 75 MHz since parallelism is most critical at shorter wave lengths. The transmitter pulse was tuned to a maximum at a given frequency. To check that the comparison pulse generator was operating at the same frequency, the two pulses were overlapped, and the comparison pulse frequency tuned until beating was observed in the oscilloscope display. It was not possible to measure the precise separation of the delay rods so the total sound absorbed, in decibels, was measured as a function of the change in separation, in centimeters. More precisely a reading was taken by selecting a value on the precision attenuators which gave a suitable height for the comparison

pulse. The transmitted pulse was matched to the same height with the micrometer drive of the mechanical system. Where possible five or more measurements of attenuation and distance were taken in replicate. The sound absorption coefficient α in decibels per centimeter for each frequency was obtained from the slope of the plot of distance versus attenuation.

CHAPTER III

STATEMENT OF THE PROBLEM

The aim of this study is the measurement and the interpretation of the ultrasonic absorption spectra of the nitrates of La(III), Ce(III), Pr(III), Sm(III), Er(III), and UO_2(II), and the sulfates of Pr(III), Sm(III), Er(III), and UO_2(II).

The sulfates of Sm[13] and Pr[14] have been studied previously by ultrasonic techniques and a comparison of the relaxation times should serve as a check of the ultrasonic apparatus.

With regard to the studies of the transition metals, it has been fairly well established that Eigen's three step mechanism[15] holds true and the low frequency relaxation observed is indeed due to step III. However, in the case of the lanthanides a firm case for the observed relaxation being linked to step III has not been established. It is therefore proposed that a number of lanthanide nitrates and, if not already measured, their corresponding sulfates be studied. If an anion independence is seen, then the mechanism according to Eigen should hold. The nitrates must be studied at relatively high concentration since the anion contributes to low absorption because of its low charge density compared to the sulfates.[16]

The kinetics of the uranyl ion have been studied extensively by Peterson[17], by Sillen [18] and by Eyring[10] according to the scheme:

$$UO_2^{2+} + H_2O \underset{k_{-1}}{\overset{k_1}{\rightleftharpoons}} UO_2OH^+ + H^+$$

$$2UO_2^{2+} + 2H_2O \rightleftharpoons (UO_2)_2(OH)_2^{2+} + 2H^+ \qquad (12)$$

$$3UO_2^{2+} + 5H_2O \rightleftharpoons (UO_2)_3(OH)_5^{+} + 5H^+$$

Very preliminary work on sound absorption of UO_2SO_4 solutions indicated that there is a relaxation between 1 and 5 MHz. If the relaxation time for hydrolysis is calculated using the value of k_{-1} derived from the theory of diffusion controlled reactions and the known value of k_1, a value of $\tau = 2.5$ megacycles is obtained. Since uranyl sulfate also forms a strong complex the observed relaxation may be due to

1) complex formation alone

2) hydrolysis alone

3) complex formation and hydrolysis together.

As a preliminary investigation, the possibility of a contribution from (1) will be considered by a comparison of the absorption spectra of uranyl nitrate, which does not complex and uranyl sulfate, which does. A more complete study would involve the dependence of the relaxation frequency on pH.

CHAPTER IV

RESULTS AND CONCLUSIONS

The attenuation of a plane progressive wave traversing a solution is given by the expression[11]

$$I = I_o \exp(-2\alpha x) \tag{13}$$

where I = sound intensity at distance x,

I_o = sound intensity at distance zero,

α = absorption coefficient of the solution.

The experimentally measured absorption is α_T and α_{xs}, due to chemical relaxation, is obtained by subtracting the solvent contribution α_{H_2O}

$$\alpha_{xs} = \alpha_T - \alpha_{H_2O} \tag{14}$$

Equation (14) implies strict additivity of absorption contributions. The addition of a solute to a solvent can decrease the observed absorption due to the solvent even in moderately dilute solutions. This means an error is introduced in treating the absorption of electrolytes in solution as the sum of the absorption due to the solvent and that due to the chemical relaxation processes. In most instances where chemical relaxation is involved, the overall absorption is considerably greater than that for the solvent alone and the error introduced is small.[16]

Measurements are expressed as absorption per wavelength $\alpha_{xs}\lambda$,

where

$$\alpha_{xs}\lambda = \frac{\alpha_{xs} C_w}{\nu} \tag{15}$$

C_w is the velocity of sound in pure water at 25°C and ν is the frequency, Tables I through X.

Relaxation curves are shown in Figures 8 through 13. The maximum may not always be observed within the available frequency range because theoretically a complete single relaxation occurs over one decade in frequency. The curve could be extrapolated to give a rough estimate of the frequency maximum; however, a more quantitative result is obtained if the equation for chemical relaxation[18]

$$\alpha/\nu^2 = \frac{A}{1+(\nu/\nu_m)^2} + B' \tag{16}$$

is used where B' is the absorption due to the solvent and A is the amplitude of the chemical absorption. Equation (16) can be rearranged to read

$$\left(\frac{\alpha}{\nu^2} - B'\right) = \frac{\alpha - B'\nu^2}{\nu_m^2} + A \tag{17}$$

which is equivalent to

$$\frac{\alpha_{xs}}{\nu^2} = -\frac{\alpha_{xs}}{\nu_m^2} + A \tag{18}$$

A plot of the left hand side versus α_{xs} gives $-1/\nu_m^2$ as the slope and therefore the characteristic relaxation frequency ν_m, e.g. Figure 14, 15 and 16.

TABLE I

MEASURED ABSORPTION OF $Pr_2(SO_4)_3$ AT 25°C

0.00537 F

$\nu \times 10^{-6}$ (Hz)	α_T (db/cm)	α_{xs} (db/cm)	$\alpha_{xs}/\nu^2 \times 10^{16}$ (db x sec^2/cm)	$\alpha_{xs}\lambda \times 10^3$ (db)
5	0.367	0.259	103.5	7.74
15	1.699	1.306	58.0	13.02
25	3.461	2.298	36.8	13.75
35	4.867	2.640	21.5	11.29
55	8.486	3.054	10.1	8.31
75	11.358	3.340	5.9	6.66

0.00269 F

$\nu \times 10^{-6}$ (Hz)	α_T (db/cm)	α_{xs} (db/cm)	$\alpha_{xs}/\nu^2 \times 10^{16}$ (db x sec^2/cm)	$\alpha_{xs}\lambda \times 10^3$ (db)
5	0.268	0.160	63.8	4.77
15	1.095	0.701	31.2	6.99
25	2.296	1.132	18.1	6.77
35	3.438	1.211	10.0	5.18
55	6.818	1.386	4.6	3.77
75	9.510	1.492	2.7	2.98

0.00134

$\nu \times 10^{-6}$ (Hz)	α_T (db/cm)	α_{xs} (db/cm)	$\alpha_{xs}/\nu^2 \times 10^{16}$ (db x sec^2/cm)	$\alpha_{xs}\lambda \times 10^3$ (db)
5	0.199	0.091	36.4	3.73
15	0.755	0.362	16.1	3.61
25	1.673	0.509	8.1	3.05
35	2.783	0.556	4.5	2.38
55	5.988	0.557	1.8	1.51
75	8.761	0.744	1.3	1.48

TABLE II

MEASURED ABSORPTION OF $Sm_2(SO_4)_3$ AT 25°C

0.01060 F

$\nu \times 10^{-6}$ (Hz)	α_T (db/cm)	α_{xs} (db/cm)	$\alpha_{xs}/\nu^2 \times 10^{16}$ (db x sec^2/cm)	$\alpha_{xs}\lambda \times 10^3$ (db)
5	0.393	0.285	113.8	8.54
15	2.466	2.072	92.1	20.66
25	5.665	4.502	72.0	26.94
35	8.557	6.330	51.7	27.06
55	15.542	10.110	33.4	27.50
75	19.406	11.389	20.2	22.72

0.00529 F

$\nu \times 10^{-6}$ (Hz)	α_T (db/cm)	α_{xs} (db/cm)	$\alpha_{xs}/\nu^2 \times 10^{16}$ (db x sec^2/cm)	$\alpha_{xs}\lambda \times 10^3$ (db)
5	0.297	0.189	75.4	5.64
15	1.615	1.221	54.3	12.18
25	3.710	2.546	40.7	15.24
35	5.507	3.280	26.8	14.02
55	10.344	4.912	16.2	13.36
75	13.655	5.637	10.0	11.24

0.00264 F

$\nu \times 10^{-6}$ (Hz)	α_T (db/cm)	α_{xs} (db/cm)	$\alpha_{xs}/\nu^2 \times 10^{16}$ (db x sec^2/cm)	$\alpha_{xs}\lambda \times 10^3$ (db)
5	0.217	0.109	43.5	3.25
15	1.175	0.781	34.7	7.79
25	2.534	1.370	21.9	8.20
35	3.774	1.547	12.6	6.61
55	7.812	2.381	7.9	6.48
75	10.689	2.671	4.7	5.33

TABLE II (Continued)

0.00132 F				
$\nu \times 10^{-6}$ (Hz)	α_T (db/cm)	α_{xs} (db/cm)	$\alpha_{xs}/\nu^2 \times 10^{16}$ (db x sec^2/cm)	$\alpha_{xs}\lambda \times 10^3$ (db)
5	0.153	0.045	18.0	1.34
15	0.844	0.450	20.0	4.49
25	1.848	0.685	11.0	4.10
35	3.005	0.778	6.3	3.32
55	6.555	1.124	3.7	3.06
75	9.305	1.287	2.3	2.57

TABLE III

MEASURED ABSORPTION OF $Er_2(SO_4)_3$ AT 25°C

0.00539 F

$\nu \times 10^{-6}$ (Hz)	α_T (db/cm)	α_{xs} (db/cm)	$\alpha_{xs}/\nu^2 \times 10^{16}$ (db x sec^2/cm)	$\alpha_{xs}\lambda \times 10^3$ (db)
5	0.547	0.438	175.2	13.11
15	1.390	0.996	44.3	9.93
25	2.347	1.183	18.9	7.08
35	3.449	1.222	9.7	5.22
55	7.145	1.714	5.7	4.66
75	9.842	1.825	3.2	3.64

0.00270 F

$\nu \times 10^{-6}$ (Hz)	α_T (db/cm)	α_{xs} (db/cm)	$\alpha_{xs}/\nu^2 \times 10^{16}$ (db x sec^2/cm)	$\alpha_{xs}\lambda \times 10^3$ (db)
5	0.363	0.255	101.9	7.62
15	0.886	0.492	21.9	4.91
25	1.762	0.599	9.6	3.59
35	2.772	0.545	4.4	2.33
55	6.402	0.970	3.2	2.64
75	8.818	0.800	1.4	1.60

0.00135 F

$\nu \times 10^{-6}$ (Hz)	α_T (db/cm)	α_{xs} (db/cm)	$\alpha_{xs}/\nu^2 \times 10^{16}$ (db x sec^2/cm)	$\alpha_{xs}\lambda \times 10^3$ (db)
5	0.213	0.104	41.6	3.11
15	0.706	0.312	13.8	3.11
25	1.426	0.262	4.2	1.57
35	2.542	0.315	2.6	1.35
55	5.906	0.474	1.6	1.29
75	8.324	0.307	0.5	0.61

TABLE IV

MEASURED ABSORPTION OF $La(NO_3)_3$ AT 25°C

0.0545 F

$\nu \times 10^{-6}$ (Hz)	α_T (db/cm)	α_{xs} (db/cm)	$\alpha_{xs}\lambda \times 10^3$ (db)
5	0.138	0.030	8.89
15	0.870	0.476	4.75
25	2.295	1.131	6.77
35	3.776	1.549	6.62
55	8.018	2.587	7.04
75	10.861	2.843	5.67

0.0115 F

$\nu \times 10^{-6}$ (Hz)	α_T (db/cm)	α_{xs} (db/cm)	$\alpha_{xs}\lambda \times 10^3$ (db)
5	0.130	0.021	0.64
15	0.484	0.091	0.90
25	1.393	0.229	1.37
35	2.473	0.246	1.05
55	5.844	0.412	1.12
75	8.319	0.302	0.60

TABLE V

MEASURED ABSORPTION OF $Ce(NO_3)_3$ AT 25°C

0.0524 F			
$\nu \times 10^{-6}$ (Hz)	α_T (db/cm)	α_{xs} (db/cm)	$\alpha_{xs}\lambda \times 10^3$ (db)
5	0.415	0.306	9.16
15	1.181	0.787	7.85
25	2.737	1.574	9.42
35	4.701	2.474	10.57
55	9.661	4.230	11.51
75	13.173	5.155	10.28

0.0111 F			
$\nu \times 10^{-6}$ (Hz)	α_T (db/cm)	α_{xs} (db/cm)	$\alpha_{xs}\lambda \times 10^3$ (db)
5	0.180	0.071	2.13
15	0.557	0.163	1.62
25	1.347	0.183	1.10
35	2.535	0.308	1.32
55	5.910	0.478	1.30
75	8.584	0.566	1.13

TABLE VI

MEASURED ABSORPTION OF $Pr(NO_3)_3$ AT 25°C

0.0512 F

$\nu \times 10^{-6}$ (Hz)	α_T (db/cm)	α_{xs} (db/cm)	$\alpha_{xs}\lambda \times 10^3$ (db)
5	0.193	0.085	2.54
15	1.096	0.702	7.01
25	3.029	1.865	11.16
35	5.255	3.028	12.94
55	10.873	5.442	14.80
75	14.970	6.952	13.87

0.0105 F

$\nu \times 10^{-6}$ (Hz)	α_T (db/cm)	α_{xs} (db/cm)	$\alpha_{xs}\lambda \times 10^3$ (db)
5	0.152	0.043	1.30
15	0.600	0.207	2.06
25	1.540	0.377	2.25
35	2.467	0.240	1.03
55	6.152	0.721	1.96
75	8.973	0.956	1.91

TABLE VII

MEASURED ABSORPTION OF $Sm(NO_3)_3$ AT 25°C

0.0528 F

$\nu \times 10^{-6}$ (Hz)	α_T (db/cm)	α_{xs} (db/cm)	$\alpha_{xs}\lambda \times 10^3$ (db)
5	0.294	0.186	5.55
15	1.143	0.749	7.47
25	2.874	1.710	10.23
35	4.961	2.733	11.68
55	10.344	4.912	13.36
75	13.936	5.919	11.81

0.0105 F

$\nu \times 10^{-6}$ (Hz)	α_T (db/cm)	α_{xs} (db/cm)	$\alpha_{xs}\lambda \times 10^3$ (db)
5	0.112	0.004	0.11
15	0.593	0.199	1.20
25	1.541	0.378	2.26
35	2.326	0.099	0.42
55	6.256	0.825	2.24
75	8.749	0.731	1.46

TABLE VIII

MEASURED ABSORPTION OF $Er(NO_3)_3$ AT 25°C

0.0505 F

$\nu \times 10^{-6}$ (Hz)	α_T (db/cm)	α_{xs} (db/cm)	$\alpha_{xs}\lambda \times 10^3$ (db)
5	0.181	0.073	2.18
15	0.532	0.138	1.38
25	1.457	0.293	1.76
35	2.560	0.333	1.42
55	5.915	0.484	1.32
75	8.440	0.423	0.84

0.0101 F

$\nu \times 10^{-6}$ (Hz)	α_T (db/cm)	α_{xs} (db/cm)	$\alpha_{xs}\lambda \times 10^3$ (db)
5	0.141	0.033	0.98
15	0.480	0.086	0.85
25	2.274	1.110	6.65
35	2.204	0.000	0.00
55	5.478	0.046	0.12
75	8.107	0.089	0.17

TABLE IX

MEASURED ABSORPTION OF UO_2SO_4 AT 25°C

0.229 F

$\nu \times 10^{-6}$ (Hz)	α_T (db/cm)	α_{xs} (db/cm)	$\alpha_{xs}\lambda \times 10^3$ (db)
5	1.851	1.743	52.14
15	2.620	2.226	22.20
25	3.700	2.537	15.18
35	5.039	2.812	12.02
55	9.174	3.742	10.18
75	13.044	5.026	10.03

0.115 F

$\nu \times 10^{-6}$ (Hz)	α_T (db/cm)	α_{xs} (db/cm)	$\alpha_{xs}\lambda \times 10^3$ (db)
5	0.999	0.890	26.63
15	1.591	1.197	11.94
25	2.582	1.418	8.48
35	3.841	1.614	6.90
55	7.874	2.443	6.64
75	11.110	3.092	6.17

TABLE X

MEASURED ABSORPTION OF $UO_2(NO_3)_3$ AT 25°C

0.213 F

$\nu \times 10^{-6}$ (Hz)	α_T (db/cm)	α_{xs} (db/cm)	$\alpha_{xs}\lambda \times 10^3$ (db)
5	0.128	0.020	0.59
15	0.491	0.097	0.96
25	1.418	0.254	1.52
35	2.2979	0.071	0.30
55	5.833	0.401	1.09
75	8.524	0.507	1.01

0.107 F

$\nu \times 10^{-6}$ (Hz)	α_T (db/cm)	α_{xs} (db/cm)	$\alpha_{xs}\lambda \times 10^3$ (db)
5	0.112	0.004	0.12
15	0.455	0.061	0.61
25	1.388	0.225	1.34
35	2.222	0.000	0.00
55	5.535	0.103	0.28
75	8.422	0.404	0.80

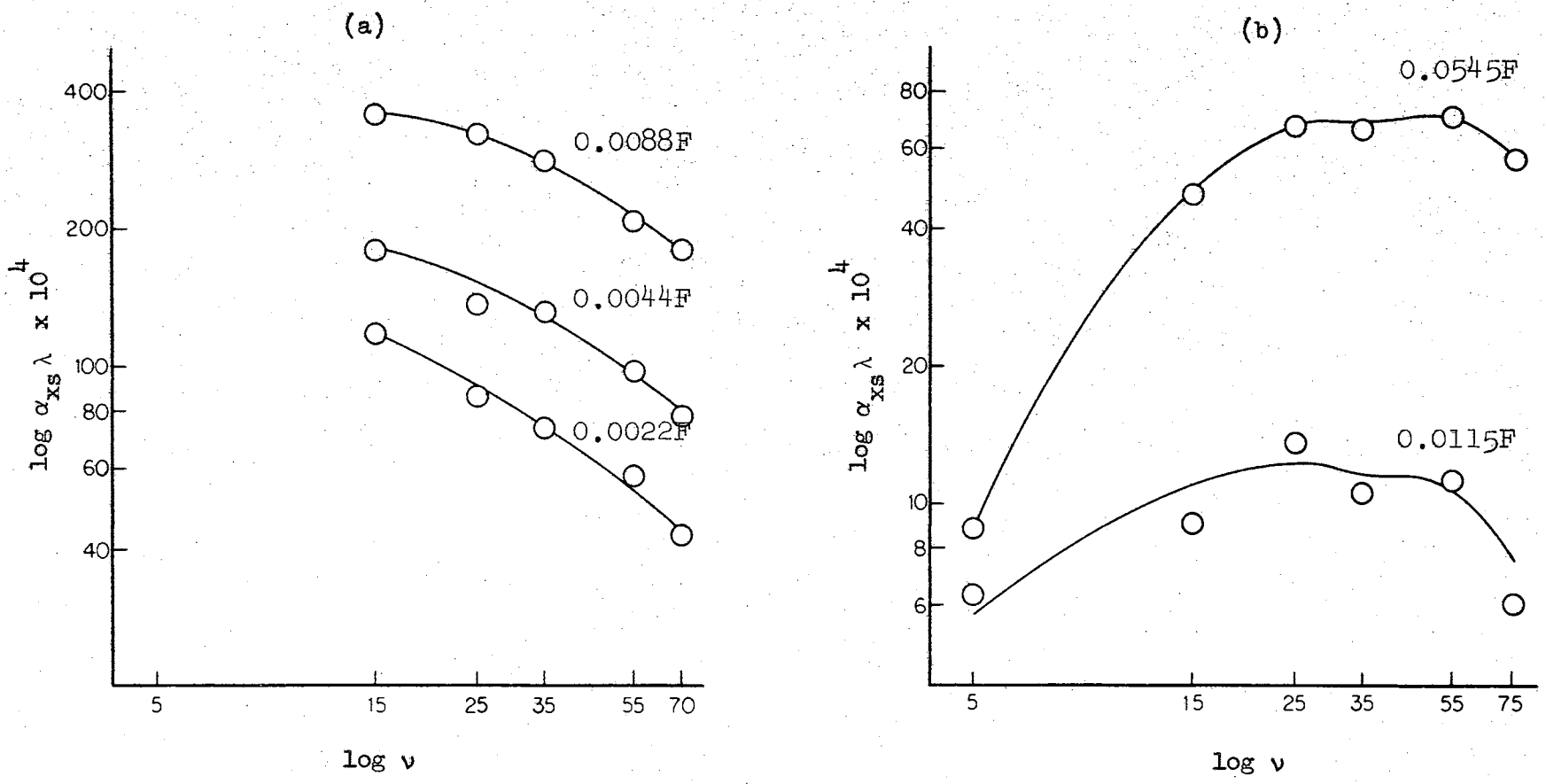

Figure 8. Sound Absorption Curves for Solutions of (a) $La_2(SO_4)_3$ and (b) $La(NO_3)_3$

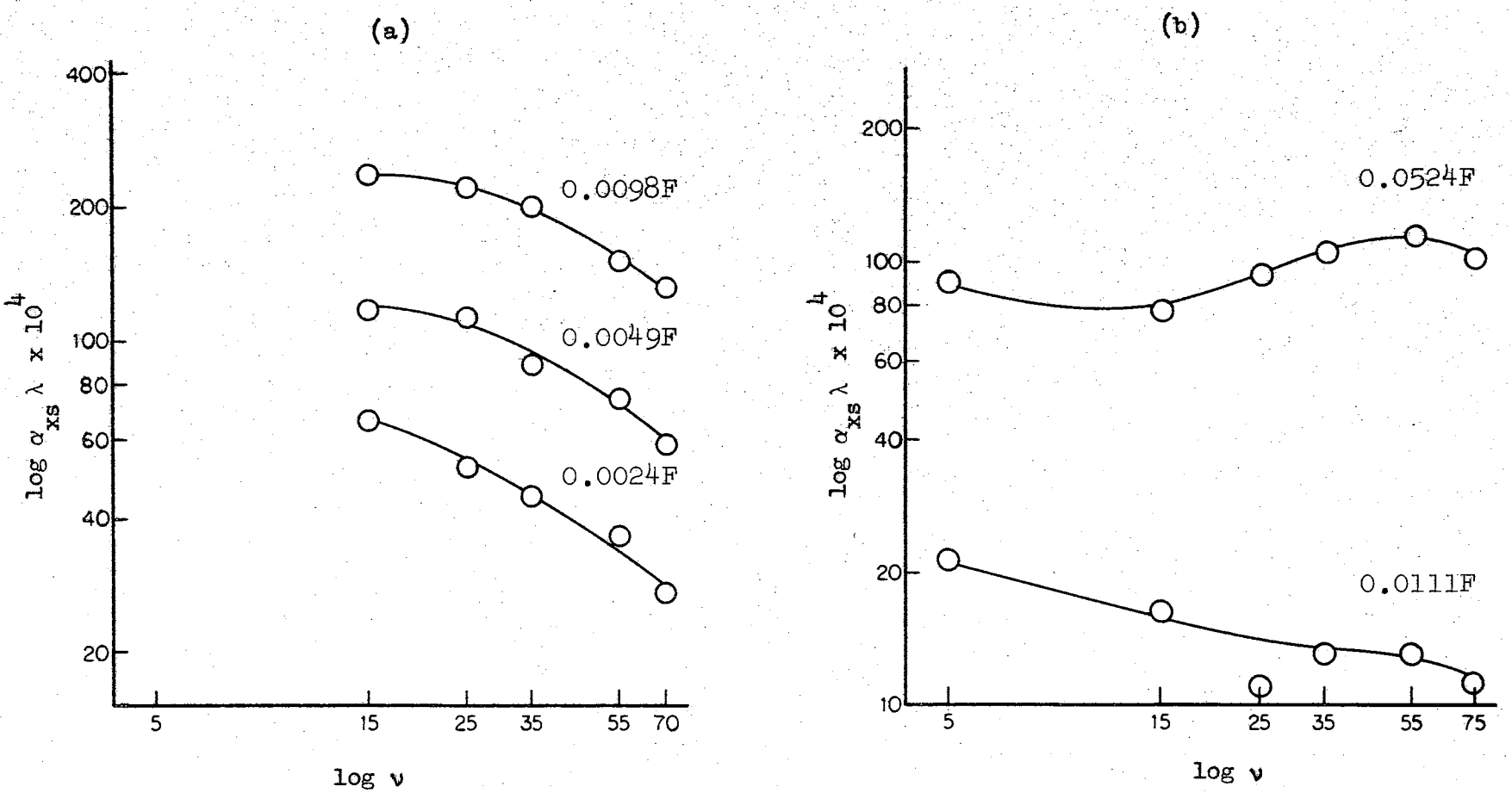

Figure 9. Sound Absorption Curves for Solutions of (a) $Ce_2(SO_4)_3$ and (b) $Ce(NO_3)_3$

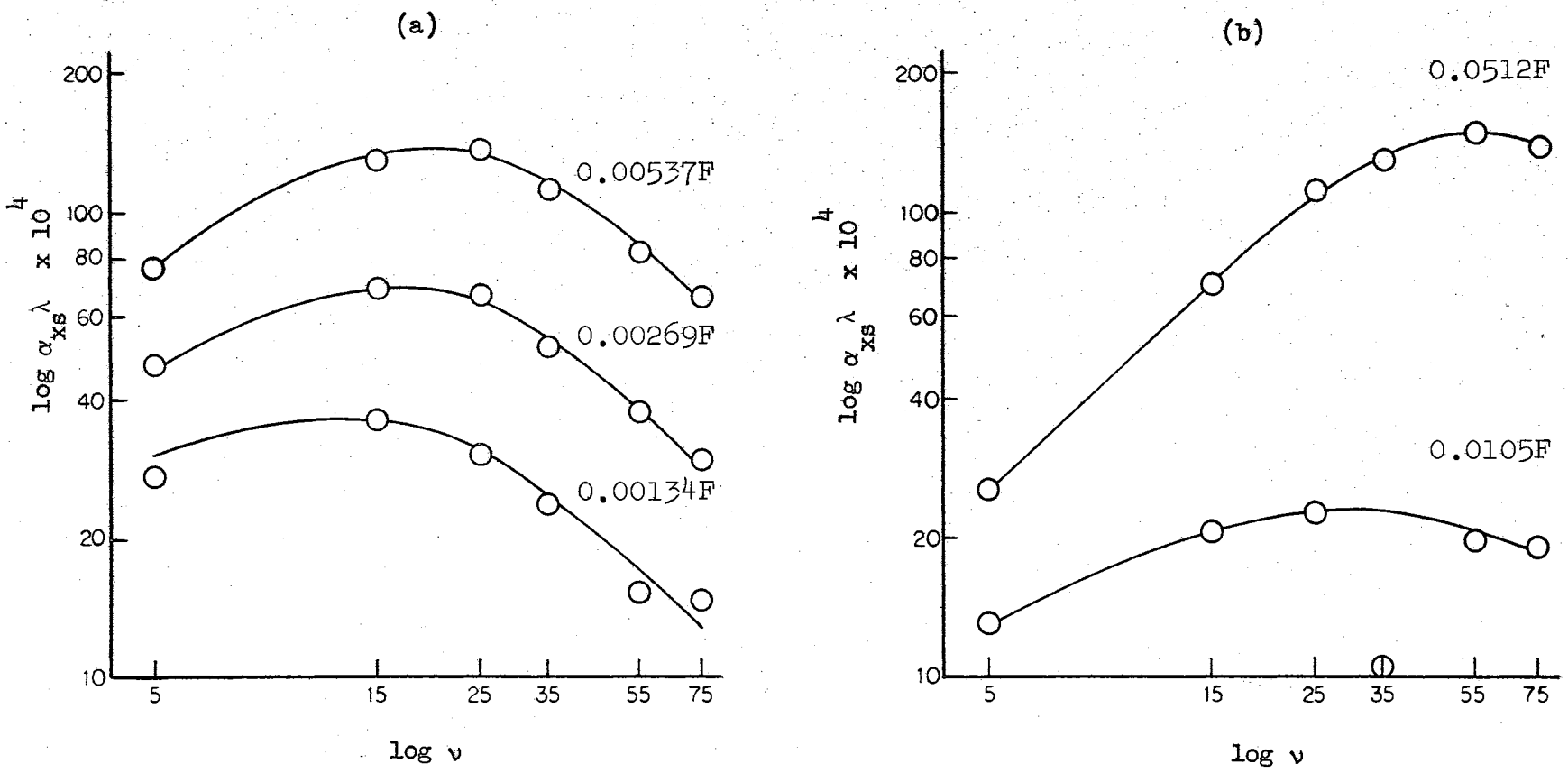

Figure 10. Sound Absorption Curves for Solutions of (a) $Pr_2(SO_4)_3$ and (b) $Pr(NO_3)_3$

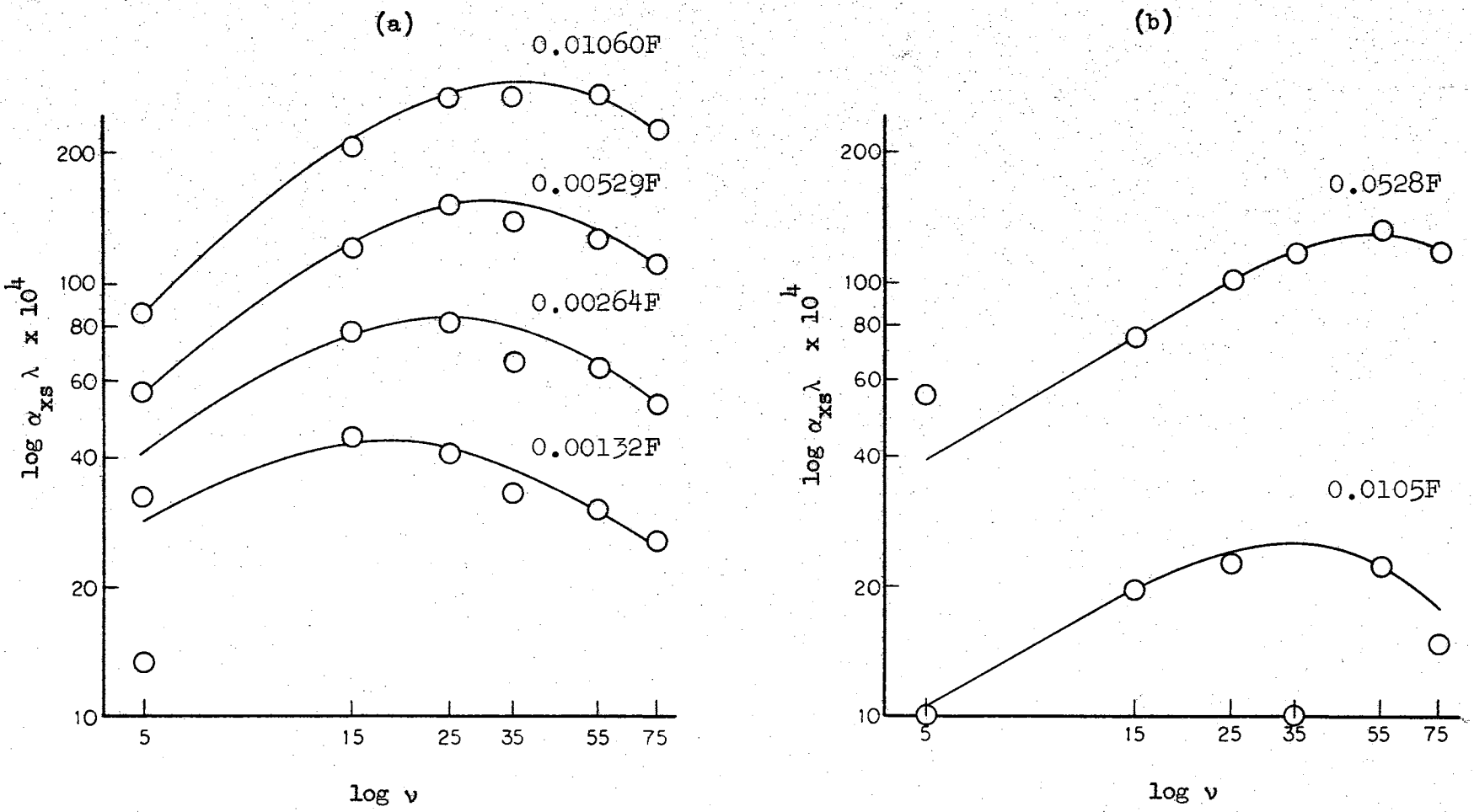

Figure 11. Sound Absorption Curves for Solutions of (a) $Sm_2(SO_4)_3$ and (b) $Sm(NO_3)_3$

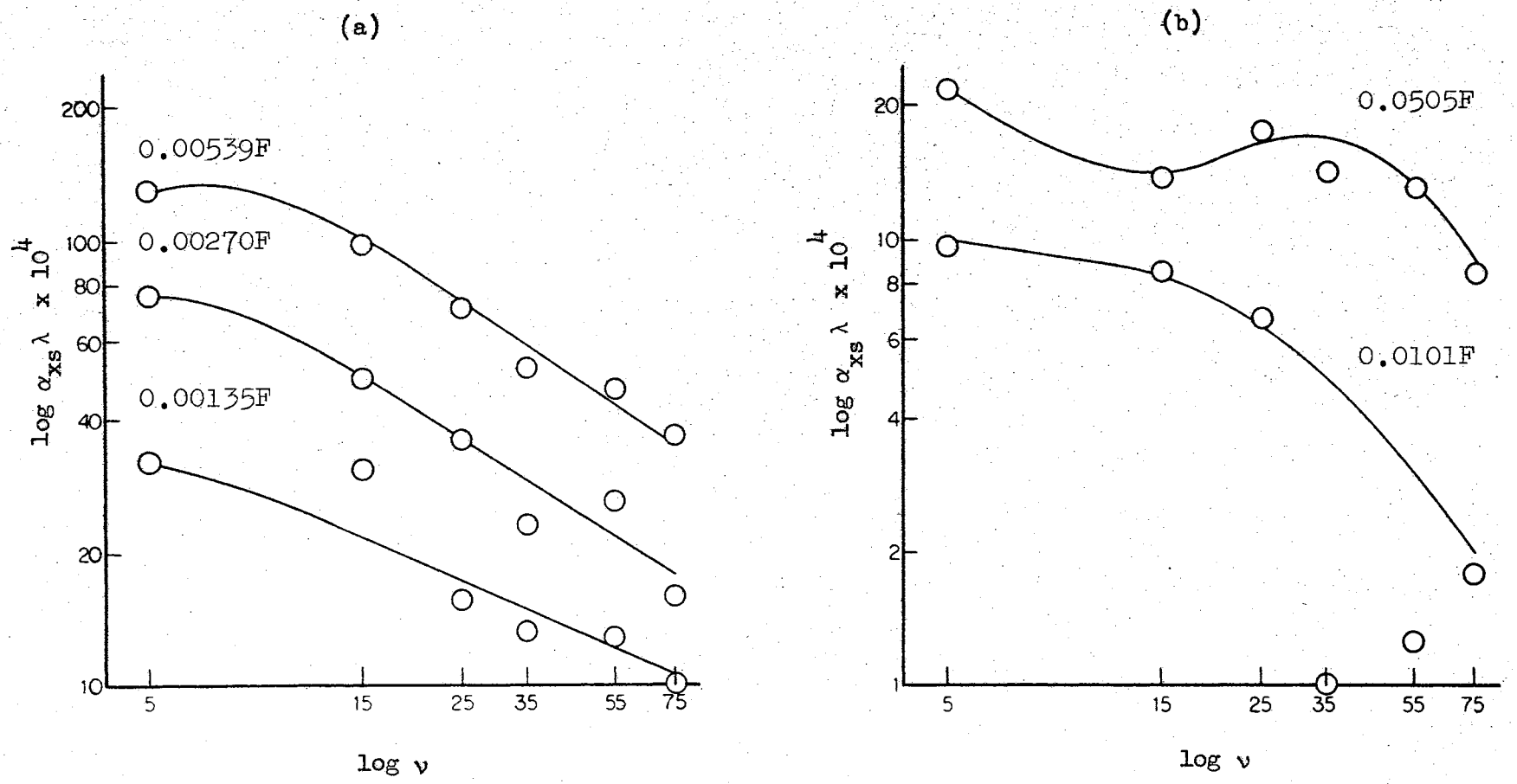

Figure 12. Sound Absorption Curves for Solutions of (a) $Er_2(SO_4)_3$ and (b) $Er(NO_3)_3$

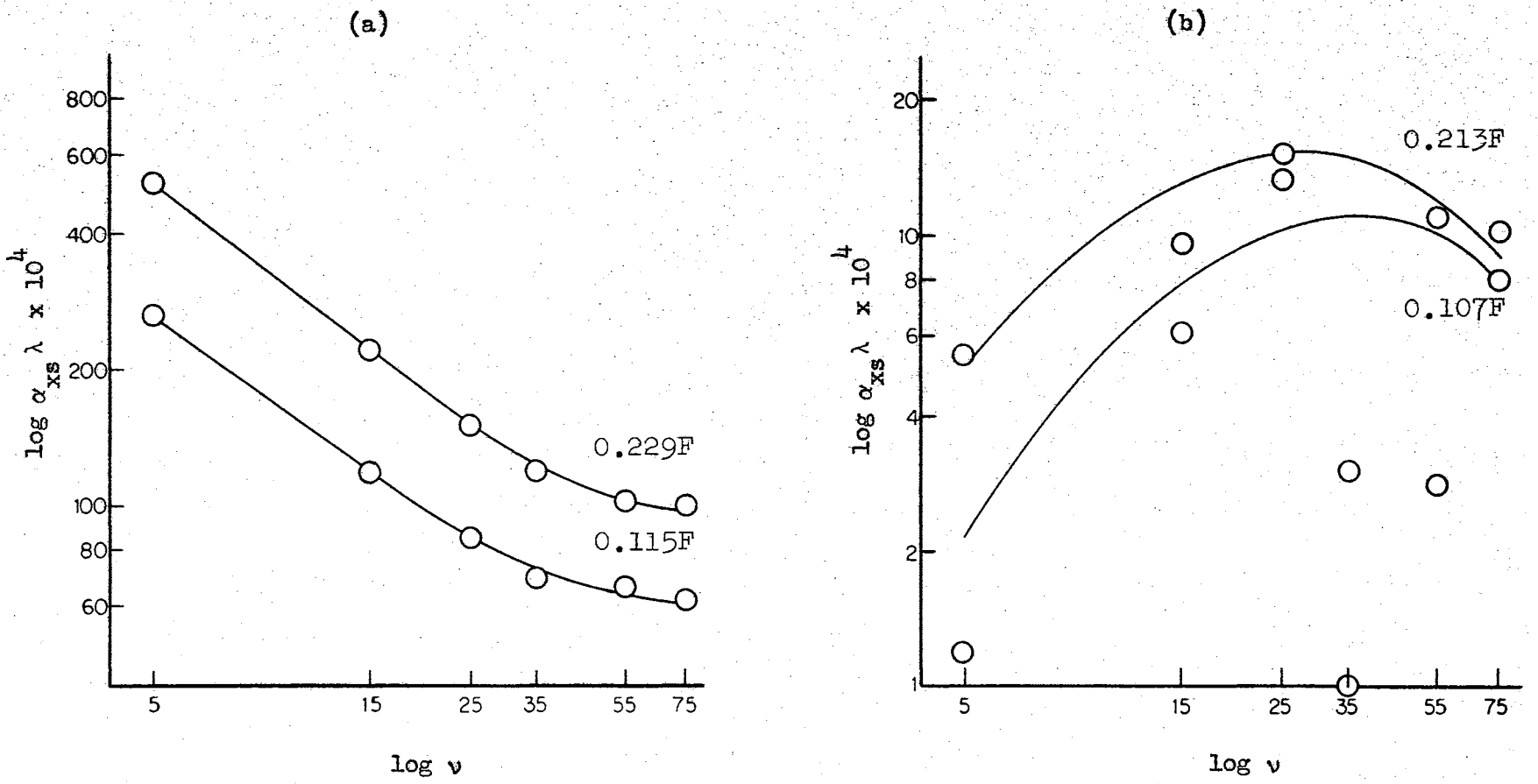

Figure 13. Sound Absorption Curves for Solutions of (a) UO_2SO_4 and (b) $UO_2(NO_3)_2$

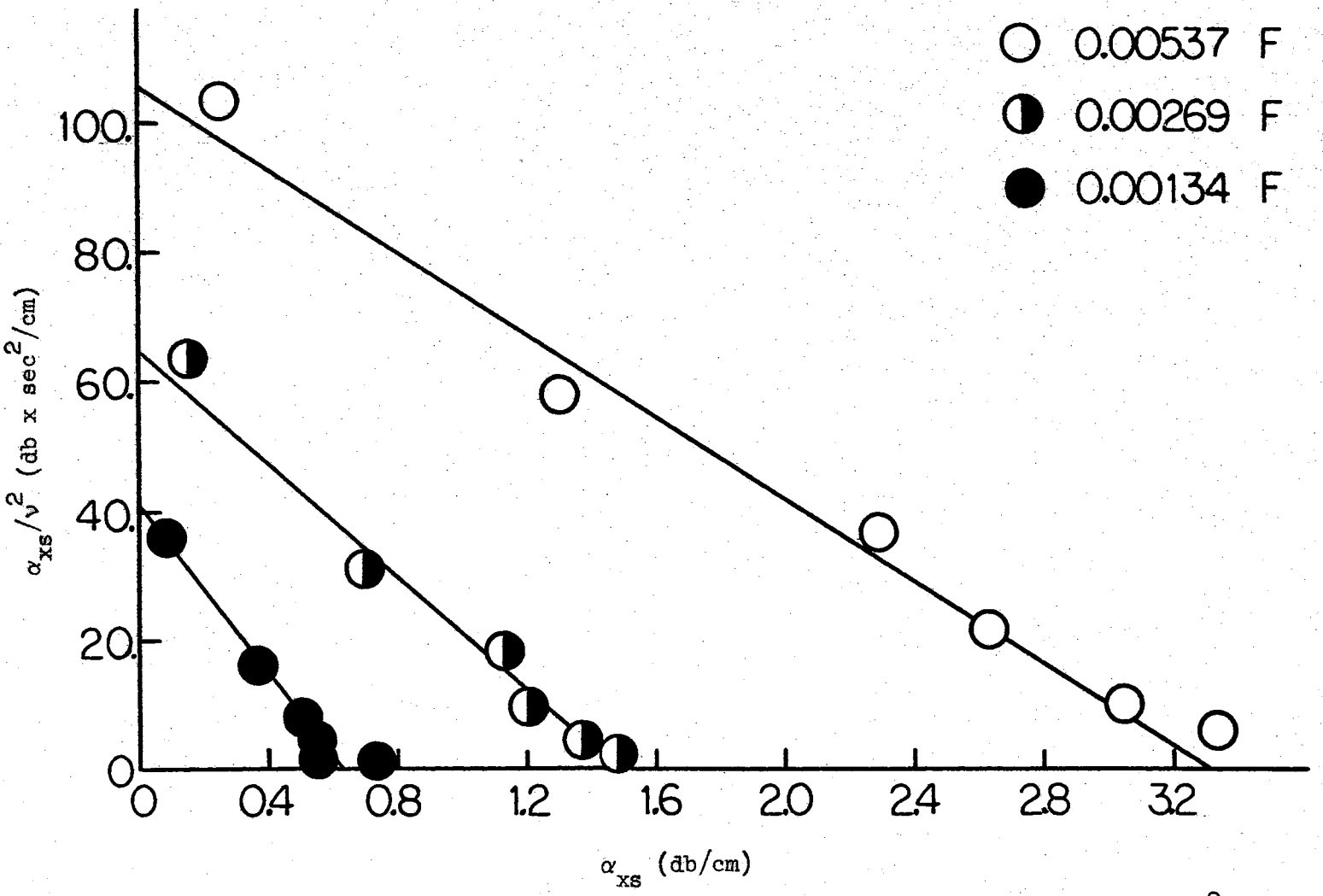

Figure 14. Plot of α_{xs}/ν^2 against α_{xs} for $Pr_2(SO_4)_3$. The slope is equal to $-1/\nu^2_{mIII}$.

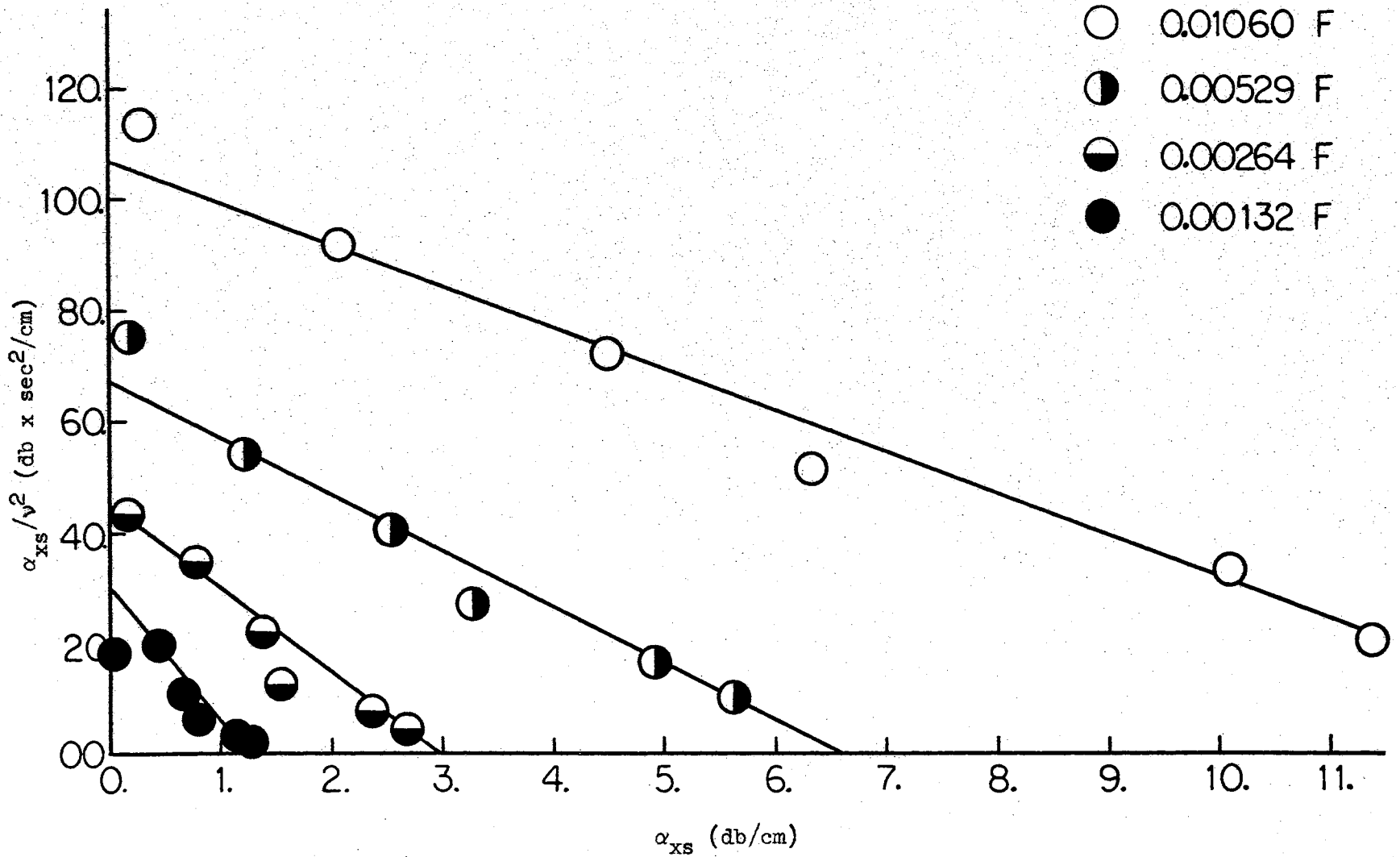

Figure 15. Plot of α_{xs}/ν^2 against α_{xs} for $Sm_2(SO_4)_3$. The slope is equal to $-1/\nu^2_{mIII}$.

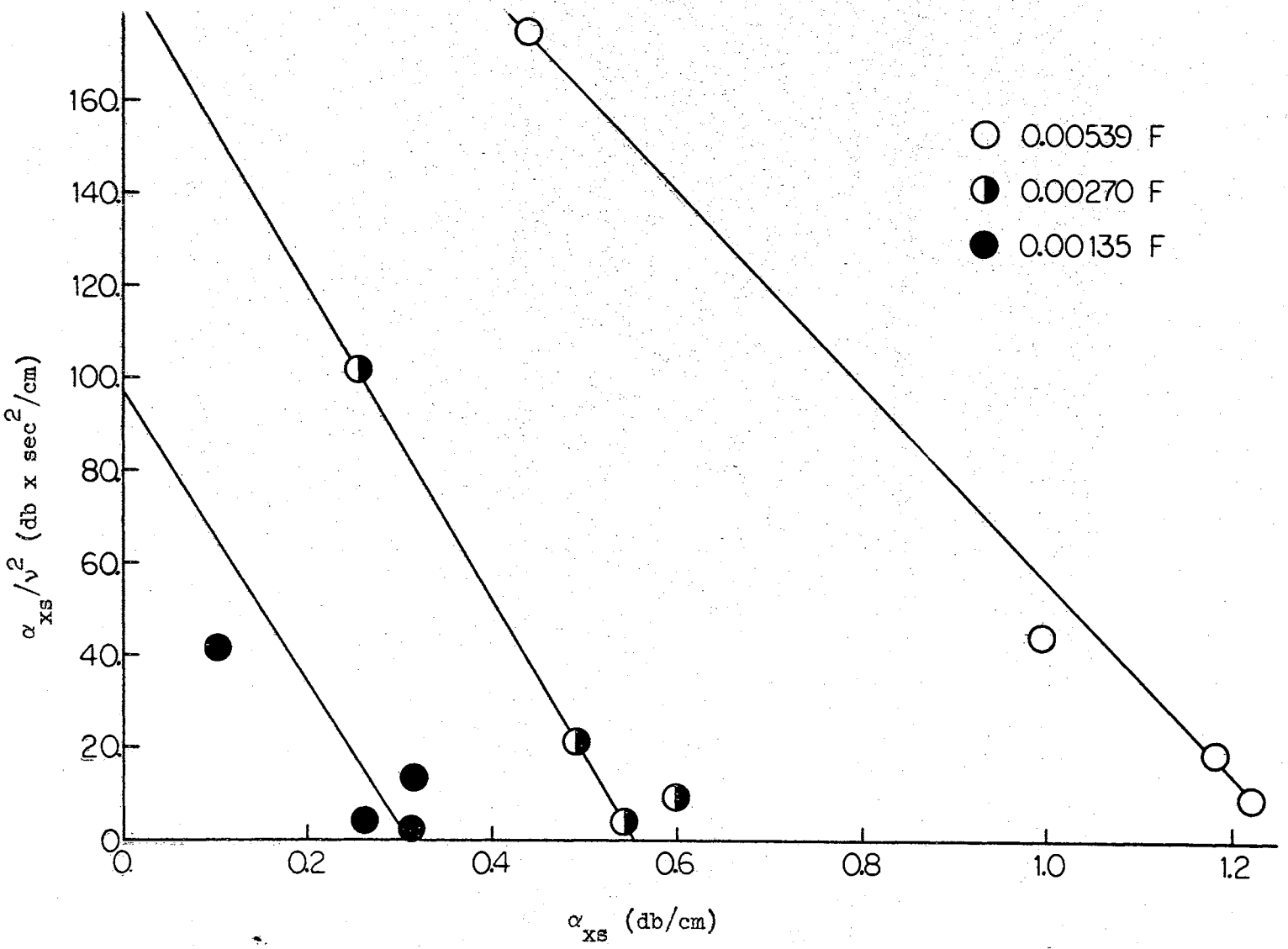

Figure 16. Plot of α_{xs}/ν^2 against α_{xs} for $Er_2(SO_4)_3$. The slope is equal to $-1/\nu^2_{mIII}$.

Lanthanide Sulfates

The analysis of the sulfates is based on the three step complex formation mechanism:[11]

$$\begin{array}{ccc} M^{3+}(aq) + SO_4^{2-}(aq) & \underset{k_{21}}{\overset{k_{12}}{\rightleftharpoons}} & [M^{3+}(H_2O)_2\ SO_4^{2-}] \\ & & \uparrow k_{32} \quad k_{23} \downarrow \\ [M^{3+}SO_4^{2-}] + H_2O & \underset{k_{43}}{\overset{k_{34}}{\rightleftharpoons}} & [M^{3+}(H_2O)SO_4^{2-}] + H_2O \end{array} \tag{19}$$

For a complete kinetic solution the spectra should consist of three relaxations corresponding to the three steps of the mechanism, with corresponding relaxation times given by the equations

$$1/\tau_I = 2\pi\nu_{mI} = k_{21} + k'_{12} \tag{20}$$

$$1/\tau_{II} = 2\pi\nu_{mII} = k_{32} + \left[\frac{k'_{12}}{k'_{12} + k_{21}}\right] k_{23} = k_{32} + k'_{23} \tag{21}$$

$$1/\tau_{III} = 2\pi\nu_{mIII} = k_{43} + \left[\frac{k'_{23}}{k'_{23} + k_{32}}\right] k_{34} = k_{43} + k'_{34} \tag{22}$$

where τ_i = relaxation time and ν_{mi} = frequency of maximum absorption for step i, k'_{12} involves a correction for activities of the ions. For small perturbations

$$k'_{12} = k^{o}_{12}\ \pi_f \left\{[M^{3+}] + [SO_4^{2-}] + [SO_4^{2-}]\left(\frac{\partial \ln \pi_f}{\partial \ln [M^{3+}]}\right)\right\} \tag{23}$$

where k_{12}^{o} is the rate constant at zero ionic strength, π_f is the activity coefficient quotient $f_{3+}\, f_{2-}/f_{\pm}$ and $[M^{3+}]$ and $[SO_4^{2-}]$ represent the equilibrium free ion concentrations in solution.

The concentration of solute is C_i mole/l. of $M_2(SO_4)_3$. At equilibrium let the degree of dissociation be γ, therefore

$$LnSO_4^{+} \rightleftharpoons Ln^{3+} + SO_4^{2-} \qquad (24)$$

$$2C(1-\gamma) \qquad 2\gamma C \qquad (2\gamma+1)C$$

$$\text{and thus } 1/K_T = \frac{[2\gamma C][C(2\gamma+1)]}{2C(1-\gamma)} \cdot \pi_f \qquad (25)$$

where K_T is the thermodynamic association constant.[19] Hence equation (23) becomes

$$k'_{12} = k_{12}^{o}\, \pi_f\, C_i \left\{(4\gamma+1) + (2\gamma+1)\frac{\partial \ln \pi_f}{\partial \ln \gamma}\right\} = k_{12}^{o}\, \theta(C) \qquad (26)$$

The values of γ were evaluated using a computer program (Appendix I) for each value of C_i (Appendix II) by standard iterations procedures where the activity coefficients f_{3+}, f_{2-} $f_{\pm}$ were calculated using the Davies equation.[20]

$$-\log f_i = .509\, Z_i^{2} \left(\frac{\mu^{1/2}}{1+Ba^{\circ}\mu^{1/2}} - 0.3\mu\right) \qquad (27)$$

where Z_i is the charge on the ith ion

B is the constant $.33 \times 10^{8}$

a^{o} is the distance of closest approach of the ions

$\mu = 3C_i + 12\,\gamma C_i$, the ionic strength of the medium.

In the original treatment of the lanthanide sulfates,[13] assumptions

were made in the evaluation of the derivative in $\theta(C)$. It was decided that a more rigorous calculation was appropriate, which involved the complete solution of the derivative with a minimum of assumptions.

$$\frac{\partial \ln \pi_f}{\partial \ln \gamma} = \frac{\partial \ln \pi_f}{\partial \mu} \cdot \frac{\partial \mu}{\partial \ln \gamma} \tag{28}$$

$$= .509(Z_A^2 + Z_B^2 - Z_{AB}^2)^2 \left[\frac{1}{2\mu^{1/2}(1+Ba^\circ\mu^{1/2})} - .3\right] \gamma C_i$$

In the original treatment of the data, the Davies equation[20] was used without modification for the ion size. B a° = 1 was taken where the estimated value of a°, the distance of closest approach of the ions, was taken as 3 Å which is too small for a 3:2 electrolyte. The new value of the distance of closest approach was taken to be the sum of the ionic radii plus two water molecule diameters. This distance varies little from cation to cation with the lanthanide series and the value a° = 8.86 Å is used for all three salts.

Activity corrections cancel in step II and III for the singly charged species. The rate expression can be written in terms of concentration and equilibrium constants

$$2\pi\nu_{mI} = k_{21} + k_{12}^\circ [\theta(C)]$$

$$2\pi\nu_{mII} = k_{32} + \left[\frac{\theta(C)}{K_{12} + \theta(C)}\right] k_{23} \tag{29}$$

$$2\pi\nu_{mIII} = k_{43} + [\theta(C)/(K_{12}K_{23} + (1+K_{23})\theta(C)] k_{34}$$

$$= k_{43} + \phi(C)\, k_{34}$$

where K_{12}, K_{23} and K_{34} are thermodynamic equilibrium constants for

TABLE XI

CALCULATION OF $\phi(C)$ FOR RARE EARTH SULFATES

$a^{o} = 8.86$ Å $\quad K_{12} = 0.0023$ mole $l.^{-1}$ $\quad K_{23} = 0.51$ unitless

Salt	C	γ	π_f	μ	$\frac{\partial \ln \pi_f}{\partial \ln \gamma}$	$\theta(C)$	$\phi(C)$
$Pr_2(SO_4)_3$	0.00537 F	0.1256	0.2463	0.0242	- 0.138	0.00176	0.459
	0.00269 F	0.1743	0.3110	0.0137	- 0.163	0.00123	0.406
	0.00134 F	0.2381	0.3839	0.0079	- 0.175	0.00087	0.350
$Sm_2(SO_4)_3$	0.01060 F	0.0822	0.1967	0.0421	- 0.095	0.00253	0.507
	0.00529 F	0.1173	0.2503	0.0233	- 0.132	0.00173	0.457
	0.00264 F	0.1636	0.3162	0.0131	- 0.157	0.00121	0.403
	0.00132 F	0.2251	0.3900	0.0075	- 0.169	0.00085	0.347
$Er_2(SO_4)$	0.00539 F	0.1333	0.2437	0.0248	- 0.144	0.00177	0.461
	0.00270 F	0.1840	0.3078	0.0140	- 0.170	0.00125	0.408
	0.00135 F	0.2499	0.3802	0.0081	- 0.181	0.00089	0.353

steps I, II and III respectively and defined by $K_{12} = k_{21}/k^{o}_{12}$, $K_{23} = k_{32}/k_{23}$, and $K_{34} = k_{43}/34$.

The value of K_{12} is calculated from the theory of diffusion controlled reactions using Bjerrum's equation[21]

$$K_{12} = \frac{4\pi N r_{AB}^{3}}{1000} b^{3} Q(b) \tag{30}$$

where $r_{AB} = a^{o}$ the distance of closest approach of the ions[22]

$$Q(b) = \int_{2}^{b} e^{b} b^{-4} db$$

$$b = \frac{Z_A Z_B}{r_{AB} Dk T} \tag{31}$$

The value obtained is .0023 mole l^{-1}. No experimental value is available for K_{23} and there is no theoretical way in which it may be calculated. Consequently the K_{23} value for $MgSO_4$ is taken,[23] equal to 0.51 (unitless). While it is unlikely that the increase in charge of the cation will not have an effect on the equilibrium constants of Step II, the nature of the cation is of secondary importance in the elimination of water from the sulfate solvation sheath.

A plot of ϕ (C) versus $2\pi\nu_{mIII}$ (Appendix III) gives k_{34} (Figure 17) as the slope and k_{43} as the intercept. The evaluation of k_{43} is complicated by the limiting value of ϕ(C) which is not zero at zero absorption. Plots of α/ν^{2}_{mIII} vs ϕ(C) for each salt were extrapolated to $\alpha/\nu^{2}_{mIII} = 0$. From plots of ϕ (C) vs $2\pi\nu_{mIII}$ the intercept at the limiting value of ϕ (C) is taken as the value of k_{43}.

The values for k_{34} and k_{43} are given in Table XII

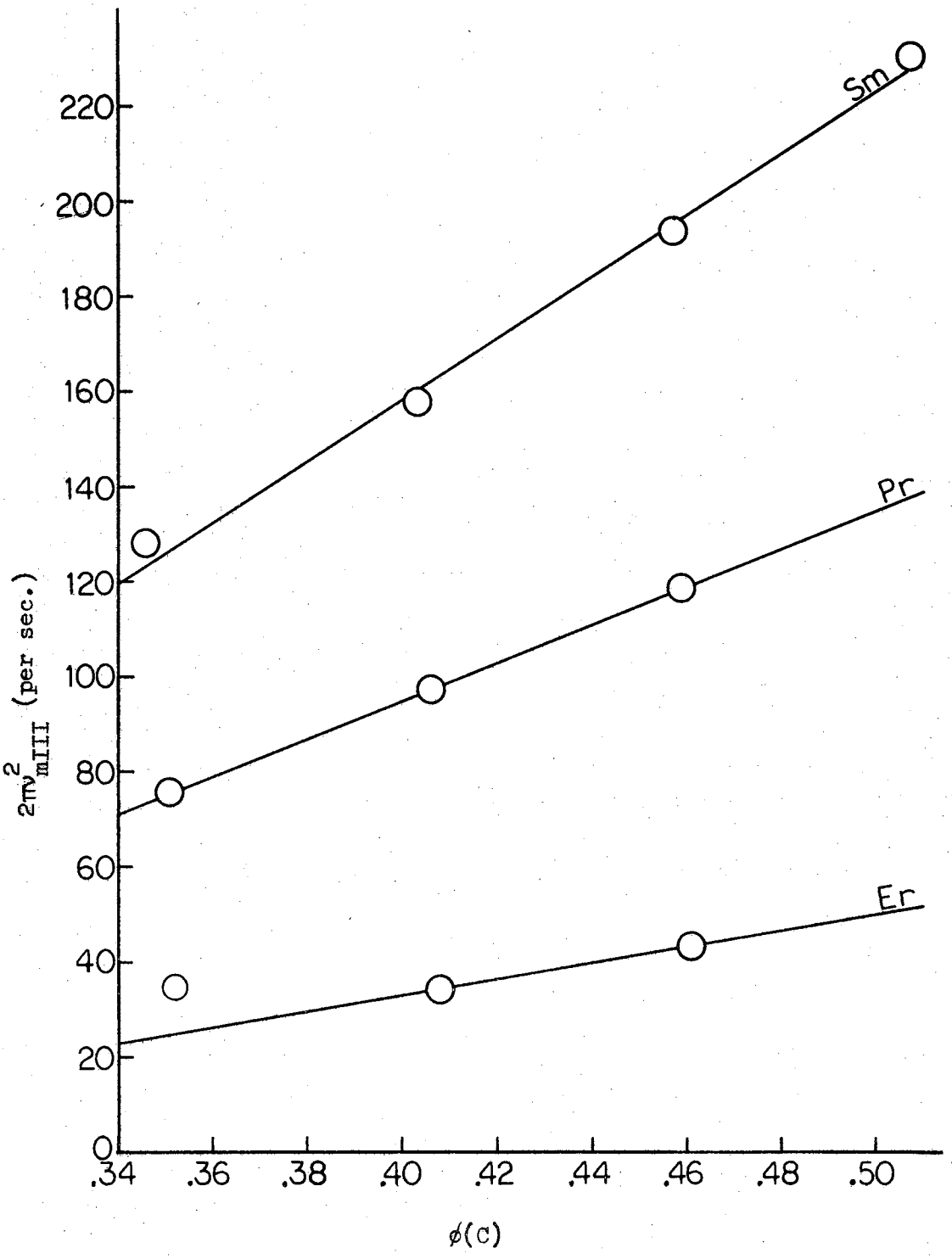

Figure 17. Plots of $2\pi\nu_{mIII}$ against ϕ(C) for the Sulfates of Pr(III), Sm(III), and Er(III).

TABLE XII

VALUE OF THE RATE CONSTANTS k_{34} AND k_{43}

Ln(III)	$k_{34}(sec^{-1})$	$k_{43}(sec^{-1})$	$1/r(\overset{o}{A}^{-1})$
Pr	4.5×10^8	5.4×10^7	0.917
Sm	6.5×10^8	9.3×10^7	0.962
Er	1.7×10^8	1.6×10^7	1.042
La	2.1×10^8	4.0×10^7	0.870
Ce	3.4×10^8	4.5×10^7	0.901
Eu	6.5×10^8	9.4×10^7	0.970
Gd	6.3×10^8	7.9×10^7	0.980
Dy	4.3×10^8	1.9×10^7	1.010
Yb	1.0×10^8	3.8×10^7	1.064

Error $\pm$ 15% on k_{34} and k_{43}

together with the recalculated values for La(III), Ce(III), Eu(III), Gd(III), Dy(III), and Yb(III) from previous work by Purdie and Vincent.[13] There is excellent agreement between the samarium results and with the praeseodymium results obtained by Grecsek.[14]

The rates of substitution are faster than those reported by Geier[7] for the murexide system by T-jump but this is not unreasonable because of the difference in ionic strength in the two systems. On the other hand the rate of water exchange (by ^{17}O NMR studies[24]) into the primary solvation sphere of gadolinium is given to be $9 \pm 2 \times 10^8$ seconds^{-1}, in excellent agreement with the present result.

In Figure 18, log k_{34} is plotted as a function of 1/r, the reciprocal cationic crystal radius. The dependence is quite different from that of Geier (Figure 4) and is non-linear which is inconsistent

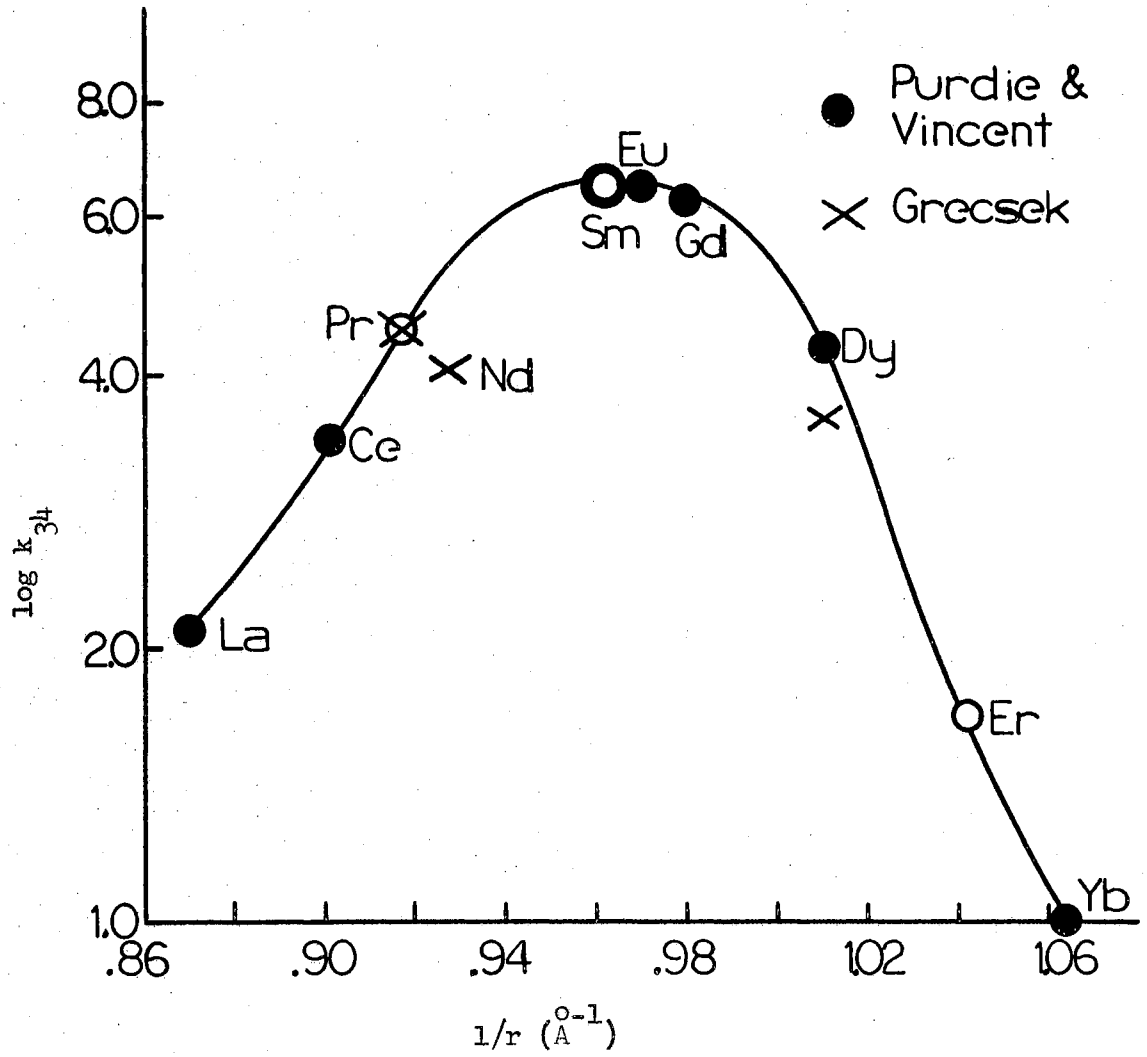

Figure 18. Dependence of log k_{34} on the reciprocal cationic radius.

with the data for the alkaline earths. In view of the weight of thermodynamic evidence for a change in coordination number within the series, it is possible that this could be used to explain the trend in rates of substitution.

The Lanthanide Nitrates

Interpretation of the lanthanide nitrates spectra is complicated by the presence of more than one relaxation. Quantitative interpretation is prohibited by inadequate theory for the resolution of multiple relaxations. The differences in the spectra, both from the corresponding sulfates and from each other, allow a qualitative description to be made.

The absorption curves are compared in Figure 8 through 13 for the sulfates and the nitrates of each particular cation. The curves differ in three respects:

(1) although sulfate solutions of equal concentration absorb to the same order of magnitude, a comparison between nitrates shows an order of magnitude difference, Table XIII.

(2) the low frequency maximum of the sulphates has been shifted to a higher value in all cases except erbium

(3) in the nitrates where the peaks have been shifted upfield, the peaks are considerably broadened as compared to a typical relaxation in the corresponding sulfate.

TABLE XIII

ABSORPTION PEAK MAXIMA

Salt	Sulfate* $(\alpha_{xs}\lambda)_{max}$ (db)	Nitrate** $(\alpha_{xs}\lambda)_{max}$ (db)
La	0.0120°	0.0070
Ce	0.0120°	0.0115
Pr	0.0190	0.0145
Sm	0.0155	0.0130
Er	0.0140°	0.0022

* ≈0.0050 F
** ≈0.050 F
° peaks are not complete

The basis for the interpretation of the sulfate data was that the relaxation was simple and due to the third step in the mechanism only i.e. the formation of the inner complex. Marcus[25] has reported that nitrates form very little inner complex unless concentrations are relatively high. The sulfates on the other hand are almost 90% inner complex. Since the amplitude of absorption depends on the concentration of inner complex and since the characteristic frequency for step III is independent of the anion, a large decrease in absorption would be expected in going to the nitrates. This is indeed true for lanthanum and erbium. An absorption at a higher frequency is also observed with some overlap of the low frequency relaxation. Since

step III is the rate determining step, this higher frequency relaxation has been identified with step II, i.e. solvent substitution into the anion. Preliminary work on calcium nitrate which is not inner-complexed shows an absorption in the frequency range 35 to 55 MHz.

For multiple relaxations, the absorptions appear separately if the characteristic frequencies differ by at least a decade.[11] When relaxations overlap, the total absorption expressed as $\alpha_{xs}\lambda$ is not simply the sum of the two values for the separate relaxations but always much larger.[26] In addition if the absorption extends over more than one decade then the characteristic frequency is shifted. The higher frequency relaxation for lanthanum and erbium occurs around 35-55 MHz and is sufficiently far removed from the low frequency relaxation in the sulfates that the curve is partially resolved.

On the other hand for cerium, praeseodymium and samarium the differences in the characteristic frequencies are much less so that overlap is substantial and no resolution is observed. Consequently the magnitude of absorption is greater for these three ions and the characteristic frequency is shifted upfield.[26]

It can therefore be concluded that the interpretation of the sulfate data is correct and the relaxations observed in the sulfates are due to the third step.

Uranyl Nitrate and Uranyl Sulfate

No valid interpretation of the data (see Figure 13) can be made. Since the absorption at 5 MHz, seen in the sulfate, is absent in the nitrate, then the principle contribution to the relaxation would appear to be due to inner sphere complex formation. Considerably more

study would have to be done to substantiate this conclusion.

BIBLIOGRAPHY

1. Frank, H. S. and W. Wen, Disc. Far. Soc., 24, 133 (1957).

2. Nancollas, G. H., "Interaction in Electrolyte Solutions," Elsevier Publishing Co., London, 1966.

3. Eigen, M. and R. G. Wilkins, "Mechanisms of Inorganic Reactions," Advances in Chemistry, No. 49, American Chemical Society, Washington, D. C., 1965, pp. 55-67.

4. Smithson, J. and T. Litovitz, J. Acoust. Soc. Am., 28, 462 (1956).

5. Connick, R. E. and E. D. Stover, J. Phys. Chem., 65, 2075 (1961).

6. Dunn, T. M., "Modern Co-ordination Chemistry," J. Lewis and R. G. Wilkins, Ed., Interscience, N.Y., 1960, p. 286.

7. Geier, G., Ber. Buns. Ges., 69, 617 (1965).

8. Yatsimirskii, K. B., Helv. Chim. Acta, Alfred Werner Commemoration Volume, 1967, pp. 166-173.

9. Hurwitz, P. and G. Atkinson, J. Phys. Chem., 71, 4142 (1967).

10. Whittaker, M. P., E. M. Eyring and E. Dibble, J. Phys. Chem., 69, 2319 (1965).

11. Eigen, M. and L. De Maeyer, "Technique of Organic Chemistry," Vol. VIII, Part II, A. Weissberger, Ed., Interscience, N.Y., 1963, Chapter 18.

12. Hammes, G. G., Science, 151, 1507 (1966).

13. Purdie, N. and C. A. Vincent, Trans. Far. Soc., 63, 2745 (1967).

14. Grecsek, J. J., Master Thesis, University of Maryland, College Park, Maryland, 1966.

15. Eigen, M., Disc. Far. Soc., 24, 25 (1957).

16. Stuehr, J. and E. Yeager, "Physical Acoustics," Vol. II, Part A, Mason, Ed., Academic Press, N.Y., 1965, p. 388.

17. Ahrland, S., S. Hietanen and L. G. Sillen, Acta Chem. Scand., 8, 1907 (1954).

18. Peterson, A., Acta Chem. Scand., 15, 101 (1961).

19. Martell, A. E. and L. G. Sillen, "Stability Constants," Special Publ. #17, Chem. Soc., London, 1964.

20. Davies, C. W., "Ion Association," Butterworths, London, 1962.

21. Robinson, R. A. and R. H. Stokes, "Electrolyte Solutions," 2nd Ed., Butterworths Scientific Publications, London, 1959, pp. 392-397.

22. Robinson, R. A. and R. H. Stokes, p. 549.

23. Atkinson, G. and S. K. Kor, J. Phys. Chem., 69, 128 (1965).

24. Swinehart, J. H., University of California at Davis, personal communication.

25. Abrahamer, I. and Y. Marcus, Inorg. Chem., 6, 2103 (1967).

26. Beyer, R. T., J. Acoust. Soc. Am., 29, 243 (1957).

APPENDICES

APPENDIX A

COMPUTER PROGRAM

```
C     DEGREE OF DISSOCIATION USING DAVIES EQUATION REPETITIVELY
C     THIS PROGRAMME REQUIRES ONE DATA CARD TO INITIATE THE CHARGES OF THE
C     SPECIES FOR ALL THE DATA TO BE EVALUATED.   THE SUCCEEDING CARDS
C     ALLOW A 6 CHARACTER LABEL AND THEN THE VALUES OF THE DISSOCIATION
C     CONSTANT AND CONCENTRATION
      DIMENSION GAM(3),Z(3),T(3)
   99 FORMAT(3F3.0)
  100 FORMAT(A6,4X,E10.3,10X,E10.3)
  101 FORMAT(1H0,68HTHE VALUES APPARENTLY APPLY TO A COMPLEX QUADRATIC E
     1QUATION - - HELP////)
  102 FORMAT(1H0,I3,6(4X,E16.8))
  103 FORMAT(1H0,12HFINAL ANSWER//1X,I3,6(4X,E16.8))
  104 FORMAT(1H1,48X,34HPROGRAM TO CALCULATE THE DEGREE OF//39X,55HDISSO
     1CIATION BY REPEATED APPLICATION OF DAVIES EQUATION//60X,13HDR. N.
     2PURDIE)
  105 FORMAT(1H0,21HDISSOCIATION CONSTANT,2X,E16.8,2X,11HMOLES/LITER//22
     1H INITIAL CONCENTRATION,2X,E16.8,2X,11HMOLES/LITER)
  106 FORMAT(4H0  N,15X,5HALPHA,15X,5HPI(F),6X,14HIONIC STRENGTH,11X,9H2
     1*ALPHA*C,7X,13HC*(2*ALPHA+1),7X,13H2*C*(1-ALPHA))
  107 FORMAT(1H0,18HCALCULATION NUMBER,I3,10X,8HSALT OF ,A6)
  108 FORMAT(1H1)
C     WRITTEN BY DANIEL LITCHINSKY
      WRITE(6,104)
C     READ CHARGES ON IONS
      READ(5,99)(Z(I),I=1,3)
      N=0
C     READ DATA CARDS FOR LABEL, DISSOCIATION CONSTANT AND CONCENTRATION
    1 READ(5,100)ARG,DISK,C
      IF(DISK*C.EQ.0.0)GOTO90
      ALF=1.0
      IF(((N/2)*2).NE.N) WRITE(6,108)
    5 N=N+1
      WRITE(6,107)N,ARG
      DO2J=1,3
    2 GAM(J)=1.0
      WRITE(6,105)DISK,C
      WRITE(6,106)
      K=0
    3 K=K+1
      PAL=ALF
      A=2.0*C*GAM(2)*GAM(3)
      B=GAM(2)*GAM(3)*C+GAM(1)*DISK
      R=(-GAM(1)*DISK)
      DS=B**2-4.0*A*R
      IF(DS)30,10,10
   30 WRITE(6,101)
      GOTO80
   10 ALF=(-B-SQRT(DS))/(2.0*A)
      IF(ALF)12,13,13
   12 ALF=(-B+SQRT(DS))/(2.0*A)
      IF(ALF)30,13,13
   13 T(1)=2.0*C*(1.0-ALF)
      T(2)=C*(2.0*ALF+1.0)
      T(3)=2.0*ALF*C
      DI=0.0
      DO15J=1,3
   15 DI=DI+Z(J)**2*T(J)*0.5
      BI=SQRT(DI)
      PI=GAM(2)*GAM(3)/GAM(1)
      WRITE(6,102)K,ALF,PI,DI,T(3),T(2),T(1)
      IF(ABS(ALF-PAL).LE.0.001)GOTO79
      DO20I=1,3
   20 GAM(I)=EXP((0.509*Z(I)**2*(BI/(1.0+2.924*BI)-0.3*DI))*(-2.302585))
      GOTO3
   79 WRITE(6,103)K,ALF,PI,DI,T(3),T(2),T(1)
      AA=(.509*12.0/(2.0*BI*(1.0+2.924*BI)**2)-1.84)*2.302585
      BB=ALF*C*12.0
      DIFF=(-AA)*BB
      THETA=PI*C*((4.0*ALF+1.0)+(2.0*ALF+1.0)*DIFF)
      CC=THETA/((.0023*.51)+(1.0+.51)*THETA)
      WRITE(6,109)AA,CC,DIFF,THETA
  109 FORMAT(1H0,10X,5HAA = ,E16.8,5X,5HFO = ,E16.8,5X,7HDIFF = ,E16.8,
     15X,8HTHETA = ,E16.8///)
   80 GOTO1
   90 STOP
      END
```

APPENDIX B

PREPARATION OF SOLUTIONS

Rare earth nitrates and oxides with a purity of 99.9% were purchased from the American Potash and Chemical Corporation. UO_2SO_4 and $UO_2(NO_3)_2$ were purchased from British Drug Houses Ltd. and Baker Chemical Co. respectively.

The hydrated rare earth sulfates were prepared from their corresponding oxide. The oxides were dissolved in 6N HCl and then 6N H_2SO_4 added to yield a quantitative amount of the sulfate. The rare earth sulfates were then precipitated by the addition of a large excess of ethyl alcohol. The sulfates were analyzed for cation concentration by cation exchange on Dowex 50W-X8 20-50 mesh resin made strongly acidic. The resulting solutions were titrated to the phenolphthalein end point with standardized sodium hydroxide.

The salts were weighed as the 6-hydrate for the nitrates and the 8-hydrate for the sulfates, the only exception being eribum nitrate which was weighed as the 5-hydrate. The concentrations were analyzed by cation exchange as before. Two ml aliquots of the solutions were passed through column loaded with acidic Dowex 50-W-X8 20-50 mesh exchange resin, and washed with 100 ml of deionized water. The resulting effluent was titrated with Fisher Certified 0.02N NaOH Solution Standard with the end point being observed potentiometrically using a Beckman research pH meter.

APPENDIX C

RELAXATION FREQUENCY DATA

Ion	Formal Conc x 10^2	$2\pi\nu_{mIII}$ (MHz)	$1/K_T$ (mole $l.^{-1}$)
*La^{3+}	0.88	84	2.38×10^{-4}
	0.44	69	
	0.22	60	
*Ce^{3+}	0.98	111	2.56×10^{-4}
	0.49	89	
	0.24	79	
Pr^{3+}	0.54	120	2.38×10^{-4}
	0.27	97	
	0.13	76	
Sm^{3+}	1.06	231	2.17×10^{-4}
	0.53	194	
	0.26	158	
	0.13	128	
*Eu^{3+}	0.98	228	1.89×10^{-4}
	0.49	185	
	0.25	161	
*Gd^{3+}	0.95	207	2.56×10^{-4}
	0.47	171	
	0.24	143	
*Dy^{3+}	0.97	104	2.56×10^{-4}
	0.65	93	
	0.32	70	
Er^{3+}	0.54	43	2.56×10^{-4}
	0.27	34	
	0.14	35	
*Yb^{3+}	3.57	48	2.56×10^{-4}
	1.14	39	
	0.94	41	

*Purdie & Vincent[13]

VITA

Daniel Litchinsky

Candidate for the Degree of

Master of Science

Thesis: RELAXATION STUDIES OF THE SULFATE AND NITRATE COMPLEXES OF THE LANTHANIDES AND U(VI) IN AQUEOUS SOLUTION

Major Field: Chemistry

Biographical:

Personal Data: Born in Calgary, Alberta, Canada, May 18, 1943, the son of Anne and Samuel Litchinsky.

Education: Graduated from Queen Elizabeth High School, Calgary, Alberta, Canada in 1961; received a Baccalaureate Degree in Science from the University of Alberta, Calgary, Alberta, Canada in 1965 with a major in chemistry; completed requirements for the Master of Science degree in chemistry in May, 1968.

Professional Experience: Research Assistant, Physics Department, University of Alberta, summer 1964 to summer 1965; Graduate Teaching Assistant in the Chemistry Department from September 1965 to January 1968.

Professional Societies: Member of the Chemical Institute of Canada.